A Final Report for:

ION DOPED QUANTUM WELL LASERS

DTIC
SELECTED
NOV 1 6 1995
S   D
F

Submitted under:
Contract No. F49620-93-C-0069

19951115 066

Submitted to:
Air Force Office of Scientific Research/PKA
110 Duncan Avenue, Suite B115
Bolling AFB, DC 20332-0001
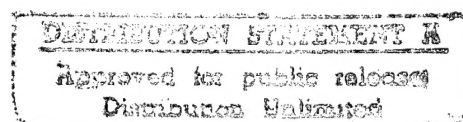
spire

Final Report for:

ION DOPED QUANTUM WELL LASERS

Date of Publication:

November 1, 1995

Sponsored by:

Strategic Defense Initiative Organization

Small Business Innovation Research Program

Issued by Air Force Office of Scientific Research

Contract No. F49620-93-C-0069

Name of Contractor: Spire Corporation

One Patriots Park

Phone: (617) 275-6000

Bedford, MA 01730-2396

Fax: (617) 275-7470

Principal Investigator: Dr. Anton Greenwald

Effective Date of Contract: September 29, 1993

Contract Expiration Date: September 29, 1995

Reporting Period: April 1 - June 30, 1995

REPORT DOCUMENTATION PAGE

Public reporting burden for this collection of information is estimated to average 1 hour per response, including the time for reviewing instructions, searching existing data sources gathering and maintaining the data needed, and completing and reviewing the collection of information. Send comments regarding this burden estimate or any other aspect of this collection of information, including suggestions for reducing this burden, to Washington Headquarters Services, Directorate for Information Operations and Reports, 1215 Jefferson Davis Highway, Suite 1204, Arlington, VA 22202-4302, and to the Office of Management and Budget, Paperwork Reduction Project (0704-0188), Washington, DC 20503

1. AGENCY USE ONLY *(Leave blank)*	2. REPORT DATE 11/6/95	3. REPORT TYPE AND DATES COVERED Final Report 9/30/93 to 9/29/95

4. TITLE AND SUBTITLE

Ion Doped Quantum Well Lasers

5. FUNDING NUMBERS

F49620-93-C-0069

6. AUTHOR(S)

Anton C. Greenwald, Ph.D.,

7. PERFORMING ORGANIZATION NAME(S) AND ADDRESS(ES)

Spire Corporation
One Patriots Park
Bedford, MA 01730-2396

8. PERFORMING ORGANIZATION REPORT NUMBER

10154

9. SPONSORING/MONITORING AGENCY NAME(S) AND ADDRESS(ES)

Air Force Office of Scientific Research/PKC
110 Duncan Avenue, Suite B115
Bolling AFB, DC 20332-0001

10. SPONSORING/MONITORING AGENCY REPORT NUMBER

11. SUPPLEMENTARY NOTES

12a. DISTRIBUTION/AVAILABILITY STATEMENT

12b. DISTRIBUTION CODE

13. ABSTRACT *(Maximum 200 words)*

The objective of this research was to fabricate erbium-doped diode lasers which were expected to be temperature independant, frequency stable sources of 1538 nm light optical communications. New metalorgainc sources of erbium were developed that enabled metalorganic chemical vapor deposition (MOCVD) of Er:GaAs and AlGaAs structures with low levels of carbon and oxygen. Substitutional doping levels to over 10^{20} per cubic centimeter were demonstrated with good photo- and cathode-liuminescence properties. LED's and diode laser structures were fabricated with erbium placed (a) so as to be pumped directly by electron-hole pair recombination, and (b) by optical absorption at 980nm. However, lasing at 1538nm was not observed in either case.

The program did result in two commercial products: the erbium metalorganic source chemicals, and laser diode arrays with 980nm emission which can be used to pump erbium-glass solid state lasers.

14. SUBJECT TERMS

diode lasers, erbium doped GaAs, rare earth doped GaAs, GaAs, AlGaAs, rare earth doped semiconductors, metalorganic erbium compounds, volatile erbium compounds

15. NUMBER OF PAGES 47

16. PRICE CODE

17. SECURITY CLASSIFICATION OF REPORT	18. SECURITY CLASSIFICATION OF THIS PAGE	19. SECURITY CLASSIFICATION OF ABSTRACT	20. LIMITATION OF ABSTRACT
Unclassified	Unclassified	Unclassified	Unlimited

SUMMARY

Solid-state diode lasers are very small, bright, inexpensive sources of coherent light but are inherently not frequency-stable with temperature changes. Typically, variations of 0.3 nm shift in average wavelength per degree Celsius change in temperature are observed. If frequency stability is required, as in matching wavelengths to fiber-optic amplifiers, relatively bulky, power consuming thermoelectric coolers are necessary.

Lasers driven by ion emission are frequency stable. The concept of electrically or optically pumping erbium ions in a semiconductor matrix for frequency stable operation is not new, but laser emission has not been demonstrated.

The objective for the first year of this program was to demonstrate metalorganic chemical vapor deposition of good quality GaAs films in-situ doped with erbium using new source materials. This objective was achieved. Prior work had demonstrated erbium doping of the GaAs lattice but with large amounts of carbon in the matrix. Spire deposited films with varying erbium concentrations, up to 30 atomic percent. Analysis by Rutherford backscattering spectroscopy showed that the maximum amount of substitutional Er in the film, was 10^{19} cm^{-3}, or 0.02 atomic percent. The films were further analyzed by secondary ion mass spectroscopy for low levels of contaminants such as carbon, oxygen, and nitrogen - all found to be negligible - and for silicon. The concentration of Si in the film varied with deposition temperature, being higher for greater deposition temperatures in the range 500 to 720°C. Photo- and cathode-luminescent spectroscopy showed narrow emission lines at 1.54 microns. Emitted power was reduced at 300K by a factor of four compared to the signal at 77K. Photoluminescence emission spectroscopy, measurement of emitted power as a function of excitation wavelength, showed that 1538 nm length from erbium in GaAs was almost entirely due to short wavelength light absorbed by the semiconductor.

Diode laser arrays designed to emit at 980 nm were fabricated and tested. Erbium was then added to a identical structure on either side of the quantum well. This erbium-device showed photoluminescence at both 970 and 1538 nm, but only 970 nm emission as an LED and no lasing activity. It is shown that the lack of laser emission may be due to the high level of oxygen concentration which accompanies the Er doping.

TABLE OF CONTENTS

LIST OF FIGURES

LIST OF FIGURES (Concluded)

LIST OF TABLES

SECTION 1

PROGRAM GOALS

The overall goal of this program was to fabricate a laser diode whose emission wavelength is stable with respect to changes in temperature. Existing semiconductor technology uses electronic transitions across the bandgap for optical emission. As the bandgap varies with temperature, a different physical mechanism must be employed for temperature invariant wavelength. As typical solid-state ionic lasers do not show the same temperature variations, Spire proposed to integrate a diode and an ionic laser in one structure (Figure 1) to achieve this goal.
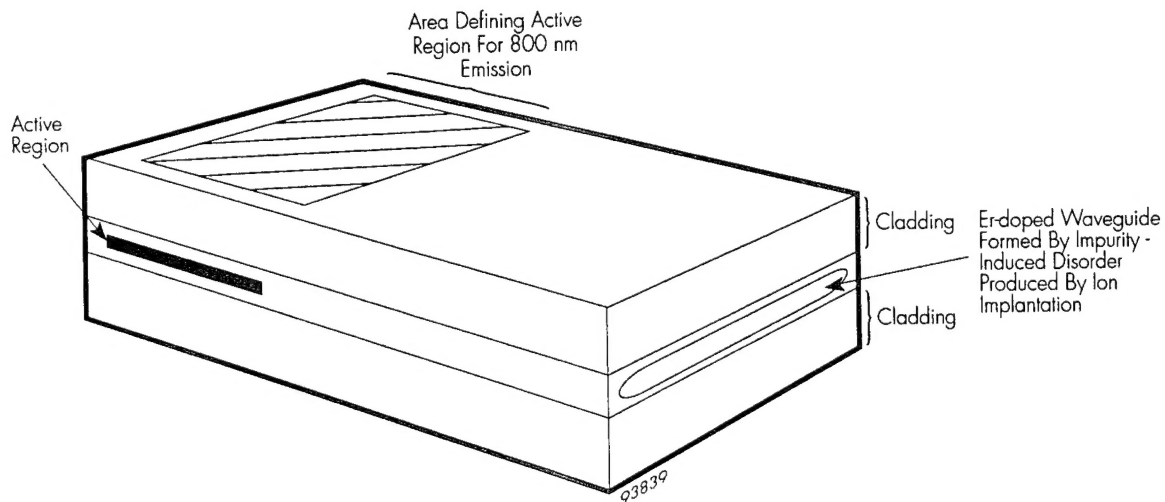
Figure 1   *Monolithic AlGaAs diode pumped erbium waveguide laser.*

It is considered theoretically possible to pump group IIIA ions in a GaAs matrix electrically, and the cross-section for such an excitation mechanism would be greater than the cross-section for optical pumping.[1] However, an electrically excited ionic laser has not been demonstrated. Only one paper reported electroluminescence of erbium doped GaAs using a reversed biased diode geometry which was inefficient and involved high voltages.[2] Many researchers have reported photoluminescence of erbium doped GaAs and Al GaAs grown by MBE[3, 4, 5] or by MOCVD.[6, 7, 8] The reduced risk approach taken by Spire assumed that high intensity light in the waveguide region of a diode laser is sufficient to pump the erbium for lasing at 1.54 microns. The design in Figure 1 allows for a reduced substitutional erbium concentration to be compensated by a longer lasing region. The actively pumped length is kept small to increase efficiency and reduce the heat load that must be removed from the device.

1

For proper lasing action, the erbium in the GaAs-AlGaAs matrix must be substitutional. An erbium ion emits 1.54 μm only when ionized to the +3 state. Interstitial erbium atoms do not have the right electron coordination. The reported solid solubility of erbium in MOCVD grown GaAs at room temperature is about $10^{19}/cm^3$, which is lower than typical concentrations in glass lasers (about $10^{20}/cm^3$). To increase gain, the length of the optically pumped 1.54 micron emission region is extended in the design of Figure 1. Information received after the start of this program indicates that this concept may not be feasible.[†]

The technical goal for the first year of this research program was to show that erbium could be incorporated substitutionally in a GaAs and AlGaAs matrix at high concentration without contaminants. Other researchers have grown such material, but with excess carbon doping.[9] Spire used new, unique chemical sources for erbium to reduce the contaminant concentration. Spire demonstrated these goals through SIMS, RBS, and Auger spectroscopy data, and also delivered two samples to AFOSR for independent verification.

The technical goal for the second year of the program was to fabricate two types of erbium doped lasers, one using direct electrical excitation for pumping the erbium ions, and one using 980nm light generated from a monolithically joined diode laser to pump the erbium ions in a GaAs matrix. Intermediate steps required to meet these goals was the demonstration of a 980nm diode laser, and a demonstration that ion implantation could be used to prevent lasing from a buried quantum well without affecting the erbium waveguide properties. Spire met both of the intermediate goals. The final devices, however, though good electrically functional diodes, did not emit light at the desired wavelength with sufficient intensity to be easily detected.

[†]   Maj. Prairie, AFOSR, private communication August 1995.

SECTION 2

DESCRIPTION OF RESEARCH

2.1   Erbium Source Synthesis

Four erbium sources were synthesized for this program, one by Gallia, Inc. and the other three by Prof. W. Rees, Jr. of Georgia Institute of Technology, the subcontractor to this program. Synthesis of the first source discovered in Phase I of this research program was covered in the final report and presented at symposia of the Materials Research Society.[10, 11]   Synthesis of other compounds is described below,[12, 13] and in additional publications.[14]

All of these compounds are air and moisture sensitive and all manipulations were performed in an inert atmosphere of dry nitrogen or argon using standard Schlenk or glove box techniques. The solvents were degassed and freshly distilled from sodium or potassium benzophenone prior to use.

2.1.1   Preparation of $Er\{N[Si(CH_2CH_3)_3]_2\}_3$

The lithium substituted amide, $LiN[Si(CH_2CH_3)_3]_2\}$ was prepared first. The reaction proceeded in a 500 ml three-necked, round-bottomed glass flask equipped with a reflux condenser, a pressure-equalizing delivery funnel, an internal magnetic stirring bar, a mercury bubbler, and a nitrogen gas inlet. Freshly titrated ^nBuLi/hexanes solution (2.5 moles/l, from Aldrich) was added dropwise to an initial solution of 24.84 g of hexaethyldisilazine $(HN[Si(CH_2CH_3)]_2$, 101.15 mmole) in 100 ml of diethylether cooled to 0°C. The reaction mixture became increasingly cloudy yielding a white precipate of the lithium salt at completion. the mixture was slowly warmed to room temperature (1 hour), refluxed for 2 hours, then stirred for an additional 2 hours at ambient temperature.

The suspension described above was placed in a 500 ml Schlenk flask, equipped with an internal magnetic stirring bar and a silicon oil bubbler, and cooled to 0°C. Erbium trichloride (9.22g, $ErCl_3$, anhydrous, 33.7 mmole, Strem Chemicals) was added through a canula as a diethylether suspension over a period of 2 hours. The erbium trichloride and the lithium salt dissolved slowly and the solution became intense pink, accompanied by a precipitation of white lithium chloride. After warming on its own to ambient temperature, followed by stirring for 24 hours, the pink solution was filtered and all volatiles were removed at a reduced pressure of about 20 - 50 torr. The residue was then treated with 200 ml of hexane and filtered from again precipitated lithium chloride. The solvent was distilled off the clear solution and yielded a pink and viscous liquid.

2.1.2   Preparation of $Er\{N[^tBu)(Si(CH_3)_3]\}_3$

A solution of 45.2 g of ^{t}butylamine $\{^tBuNH_2$, 618 mmole) in 650 ml of diethylether cooled to 0°C was prepared in a 1000 ml Schlenk flask equipped with an internal magnetic stirring bar and a silicon oil bubbler. Trimethylchlorosilane (33.5 g, $ClSi(CH_3)_3$, 309 mmole, 39.2 ml) was added very slowly through a syringe. After warming to ambient temperature, the white solid (^{t}butlyamine hydrochloride) was removed by Schlenk filtration. The remaining clear solution was distilled at

ambient pressure to yield the desired product at 118°C. The yield was 20.6 g, or 45.8% of ^{t}butly-trimrthylsilylamine or $HN\{[Si(CH_3)_3]({}^tBu)\}$.

The 20.6 g of ^{t} butyltrimethylsilylamine prepared above was dissolved in 100 ml of diethylether, placed in a smaller 250 ml Schenk flask equipped with an internal magnetic stirrer and a silicon oil bath, and cooled to 0°C. Then 56.7 ml of a freshly titrated ^{n}BuLi/hexanes solution (2.5 mole/l) was added over a period of 50 minutes. After warming on its own to ambient temperature, the pale yellow, cloudy solution was refluxed for one hour, then cooled on its own to ambient temperature. The white lithium amide, $LiN\{[Si(CH_3)_3]({}^tBu)\}$, was then purified by recrystallization from an ether/hexane solution. Total yield was 19.47 g, or 91%.

The final product was prepared in a 1000 ml, three-necked, round-bottomed flask equipped with a pressure-equalizing funnel, an internal magnetic stirring bar, a silicon oil bubbler, and a nitrogen gas inlet. This flask was initially filled with 11.74 g of anhydrous erbium trichloride ($ErCl_3$, 42.9 mmole) dissolved in 300 ml of diethylether and cooled to 0°C. All 19.47 g of the lithium amide preparation was dissolved in 100 ml of diethylether and added dropwise with rapid stirring over a period of 2 hours. The reaction solution was then warmed to ambient temperature over a period of one hour and stirred for another 12 hours at this temperature. The pink solution was filtered from lithium chloride and all volatiles were removed at reduced pressure. The pink solid residue was subsequently extracted with hexane and filtered from again precipitated lithium chloride. The remaining pink solid was then dried in vacuum (10^{-2} torr) at about 80°C over a period of 24 hours. Ensuing sublimation at 10^{-4} torr and 100°C gave the desired product, an intense pink colored amorphous powder with a yield of 12.85 g (49.9%). NMR spectroscopy results: $[C_6D_6, \delta, ppm]$, 0.875 (s, 27H, $C(CH_3)_3$); -0.016 (s, 27H, $Si(CH_3)_3$).

The structure of tris-^{t} butyltrimethylsilylerbiumamide is shown in Figure 2. Preliminary measurements of its vapor pressure at 80, 100, and 130°C are, respectively, 10^{-5}, 10^{-4}, an d 10^{-3} torr.
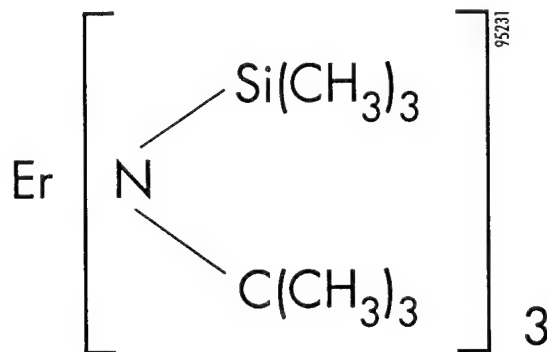
Figure 2   *Structure of tris-^{t} butlytrimethylsilylerbiumamide.*

2.1.3 Preparation of Er{N{(^{t}Bu)(SiH(CH$_3$)$_2$)]}$_3$

In a 1000 ml Schlenk flask, equipped with an internal magnetic stirring bar and a silicon oil bubbler, a solution of 47.83 g of ^{t}butylamoiine [^{t}BuNH$_2$, 654 mmole] in 700 ml of diethylether was cooled to 0°C and 30.9 g of dimethylchlorosilane [ClSiH(CH$_3$)$_3$, 327 mmole] was added very slowly through a syringe. After warming to ambient temperature, the white solid (^{t}butylamine hydrochloride) was removed by Schlenk filtration. The remaining clear solution was distilled at ambient pressure to yield the desired product, HN{[SiH(CH$_3$)$_2$](^{t}Bu)}, at 103°C with a yield of 13.23g, 30.8%.

The 13.23 g of ^{t}butyldimethylsilylamine was dissolved in 100 ml of diethylether in a 250 ml Schlenk flask with an internal magnetic stirring bar and a silicon oil bubbler cooled to 0°C. Then 40.3 ml of a freshly titrated ^{n}BuLi/hexanes solution (2.5 mole/l) was added over a period of thirty minutes. After warming on its own to ambient temperature, the pale yellow cloudy solution was refluxed for one hour, then cooled on its own to ambient temperature and stirred for an additional hour. The white lithium amide was then purified by recrystallization from an ether/hexane solution. The yield of LiN{[SiH(CH$_3$)$_2$](^{t}Bu)} was 12.52 g, 90%.

The final product was prepared in a 1000 ml, three-necked, round-bottomed flask equipped with a pressure-equalizing funnel, an internal magnetic stirring bar, a silicon oil bubbler, and a nitrogen gas inlet. This flask was initially filled with 8.32 g of anhydrous erbium trichloride (ErCl$_3$, 30.4 mmole) suspended in 300 ml of diethylether and cooled to 0°C. All 12.52 g of the lithium amide preparation (LiN{[SiH(CH$_3$)$_2$](^{t}Bu)}, 91.23 mmole) was dissolved in 100 ml of diethylether and added dropwise with rapid stirring over a period of 2 hours. The pink reaction solution was then warmed to ambient temperature over a period of one hour and stirred for another 12 hours at this temperature. The reaction mixture then was filtered from lithium chloride and all volatiles were removed at reduced pressure. The residue was subsequently dissolved in 300 ml of hexane and filtered from precipitated lithium chloride. The solvent was reduced to about 100 ml and the remaining pink crystals were washed five times with -78°C cold hexane and subsequently dried in vacuum at 10^{-2} torr and 50°C for 24 hours. The yield was 7.18 g at 42%.

2.2 Apparatus

The apparatus used for deposition of single crystal GaAs and AlGaAs layers epitaxially on matching substrates by metalorganic chemical vapor deposition (MOCVD) is shown schematically in Figure 3. The equipment is installed in a class 1000 clean room, with class 100 curtains for the loading/loading station.

The first task for this program was to modify this reactor to hold high temperature erbium sources. The added gas network was placed in an oven, indicated in Figure 3, for uniform heating of all valves. All valves have metal seals and are rated to over 350°C. Manually operated throttling valves were used to control the pressure because no suitable automated valves for such high temperature service were available. The pressure gauge had to be mounted upstream of the source bubbler, also because there are no suitable high temperature versions available. For steady operating conditions, the pressure remained stable and did not require frequent adjustment by the operator.

LEGEND

⋈	2-PORT BELLOWS VALVE (NC)	Ⓟ	PUMP
⋈	2-PORT BELLOWS VALVE (NO)	■	SUBMICRON FILTER
⋈	3-PORT BELLOWS VALVE	APC	AUTOMATIC PRESSURE CONTROLLER
✳	4-PORT BELLOWS VALVE	BO	BURN OFF
MFC	MASS FLOW CONTROLLER	⧄	THROTTLE VALVE
⊠	EMERGENCY EXHAUST VALVE	▯	PARTICLE FILTER/ COLD TRAP
⊘	CAPACITANCE MONITOR	– –	MODIFICATION
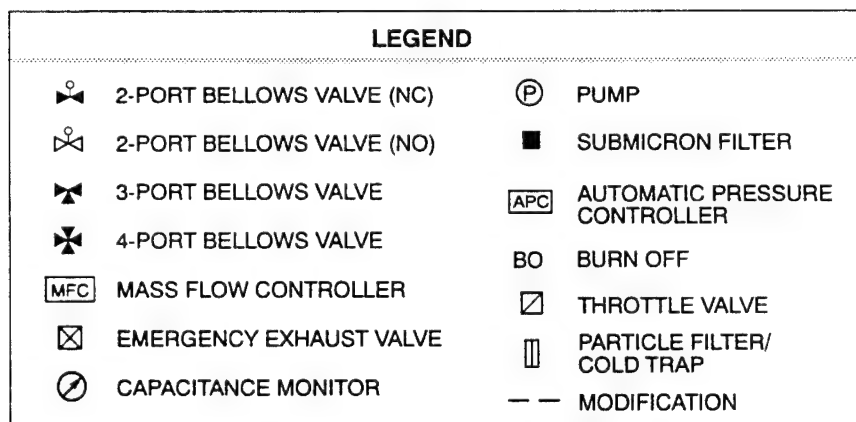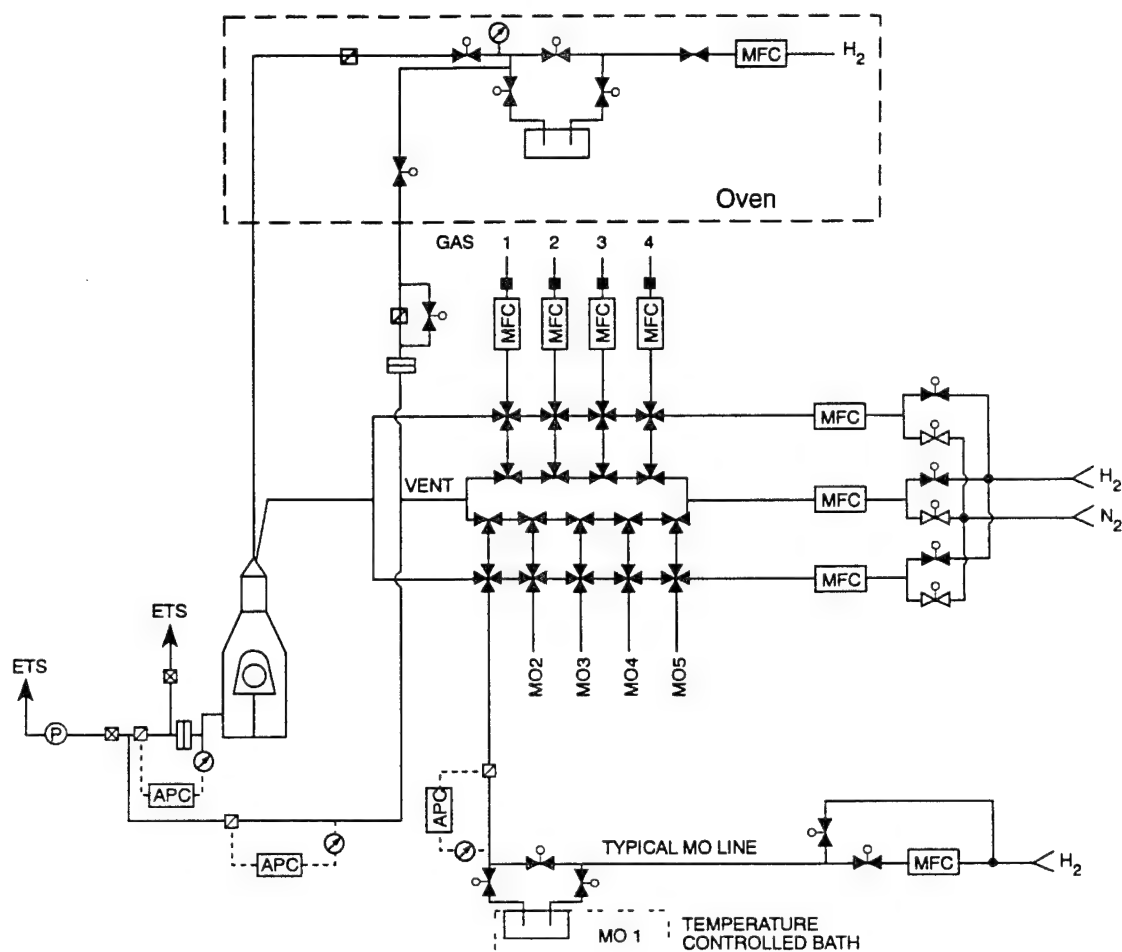
94230

Figure 3 *Schematic diagram of SPI-MOCVD™ 450 modified for this research. All parts in oven were added.*

6

2.3 Preparation and Analyses of Erbium Doped Films

Four sets of MOCVD matrix experiments were conducted to deposit erbium doped GaAs and AlGaAs films. The first experimental matrix used methylcyclopentadienyl erbium as a dopant source, the next two data sets used the tris-trimethyldisilylamido erbium source developed in Phase I of this program, while the fourth set tested a tris-triethyldisilylamido-erbium source.

2.3.1 Methylcyclopentadienyl Erbium

The designed experimental matrix for testing this source is shown in Table 1 and 2. Preliminary results with this source indicated that the concentration of erbium in a GaAs film was too low to be detected by secondary ion mass spectroscopy (SIMS) for normal growth rates. To assure that we would see erbium, the gallium source was turned off for part of the run to produce a thin layer of erbium-arsenide. The concentration spike at this point in the growth was seen by Rutherford Backscattering spectroscopy as well as SIMS.

In this experimental matrix, all substrates were half of a 2 inch diameter semi-insulating GaAs wafer. The total layer thickness includes the buffer layer which may have more to do with the final measurement than the erbium layer.

Table 1   *Time-temperature profiles for GaAs and ErAs deposition with (MeCp)₃Er.*

GaAs		Description of Deposition Steps
Temp.(°C)	Time(sec)	
100	10	purge and start arsine flow
650	600	heat up substrate, Er bypass flowing to reactor
650	15	increase arsine flow
650	120	deposit GaAs or AlGaAs buffer layer
*	900	deposit with Er and arsine only
650	30	deposit capping GaAs or AlGaAs layer
100	900	cool down
100		

*See Table 2

Samples were characterized by photoluminescence at Spire Corporation using an argon ion laser at 488 nm and an InSb detector. In addition, most samples were also characterized by secondary ion mass spectroscopy (SIMS) to determine doping levels as a function of depth and low levels of contaminants such as carbon, oxygen, nitrogen, and silicon. Rutherford backscattering spectroscopy (RBS) was used to calibrate the SIMS data for erbium content, and in the channeling mode to determine relative percentage of substitutional and interstitial erbium.

7

Table 2   *Designed experimental matrix for high Er doping with (MeCp)₃Er.*

MOCVD run #	Temp. (°C)	Press. (torr)	Total flow (slpm)	Er carrier (sccm)	AsH₃ flow (sccm)	Film thick. (μm)
1874*	650	50	4	300	175	1.2-1.5
1875*	650	50	4	300	50	.5
1876*	650	50	2	1600	50	.33
1877	650	50	2	800	50	.39
1878	650	200	5	50	50	.24-.36
1879	500	200	5	800	50	.35-.46
1880	500	50	2	50	50	.33-.46
1881	650	200	2	50	335	.33-.55
1882	650	50	5	800	335	.43-.55
1883	500	200	2	800	335	.39
1884	500	50	5	50	335	.39-.52

* deposition time for erbium layer initially 5, 5, 30, then 15 min. always

Photoluminescence data (sample 1879- see Table 2) are presented in Figure 4. The emission peak at about 1538 nm was barely above the background noise level. This reduced luminescence signal was attributed to excess erbium levels near the surface with poor crystal structure.
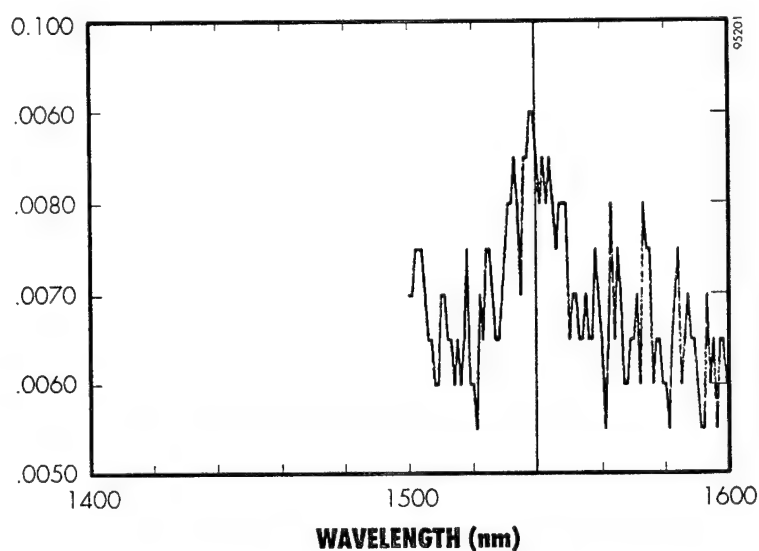
Figure 4   *Photoluminescence spectra of sample 1879 at 77K showing small peak at 1538 nm.*

SIMS data using an oxygen ion beam source from samples of run numbers 1875 through 1880 are shown in Figures 5 and 6. Data supplied by Analytical Answers Inc., Woburn MA. At high dilution (total gas flow) in the reactor, and intermediate flow through the erbium source, the concentration of erbium in the film was very low (1874, 1875). When the carrier gas flow through the erbium source was significantly increased (1876) the concentration of erbium was significantly increased. Comparing data from samples 1876, 1877, and 1879, the peak concentration for erbium in the film was roughly proportional to the carrier flow through the source. For other samples at low carrier flows, the concentration was again too low to be detected with this technique. These data implied that the amount of erbium doping in the film can be controlled by varying the flow of carrier gas through the source. Very high carrier flow rates were required for a solid source which sublimes at very low vapor pressure.

The analysis compared only the peak heights for the erbium near the surface of the sample. The erbium peak below the surface was an artifact, as discussed previously, created by a dead spot in the erbium feed line which was flushed in a "pulse" during purging of the reactor at the start of the deposition cycle. To some extenet, the height of this second, deeper peak was proportional to the settings of the erbium carrier flow.

A second measurement of erbium in sample 1879 was taken by SIMS by Charles Evans and Associates, Inc (Figure 7). This experiment used a cesium ion beam to detect carbon, nitrogen and oxygen levels in the film, but it reduced erbium signal strength (the molecular ion $ErAs^+$ was detected). Data agreed with results in Figure 5 for erbium profiles, but also showed relatively large concentrations of carbon and oxygen in the film. For comparison, carbon and oxygen profiles for a good solid-state laser wafer are shown in Figure 8. This erbium source increased contamination levels to unacceptable limits when the erbium concentration was sufficient for laser operation.

Calibration of the erbium levels in the SIMS data was determined from the RBS analysis shown in Figure 9 for sample 1879. Only one erbium peak was visible. Either the peak height of the buried layer was too small to be seen at the point where this data was taken (note linear RBS scale as opposed to a logarithmic scale for SIMS), or the signal from the two peaks was indistinguishable. The signal level from erbium was about a factor of 200 lower than the signal from Ga or As.

2.3.2   Tris-trimethyldisilylamido-erbium

This was the erbium source developed in Phase I, with a structure is similar to the amide in Figure 2 except that two trimethyl-silyl groups, $Si(CH_3)_3$, are attached to each nitrogen atom. The material was synthesized by Gallia Corporation, under license to the University of Florida. This invention, patent application in process, arose from funding for this SBIR project.

Spire purchased additional quantities of this source and in two growth runs doped GaAs and AlGaAs according to the schedule shown in Table 3. The objective of these experiments, with stepwise varying flow rates for the erbium source, was to determine how this parameter affected the level of erbium incorporated into the semi-conductor. The substrates were 2 inch diameter N^+ (1.7 to 2.8 x 10^{18} Si/cm^3) GaAs wafers. The surface of the completed structure was not perfectly smooth.
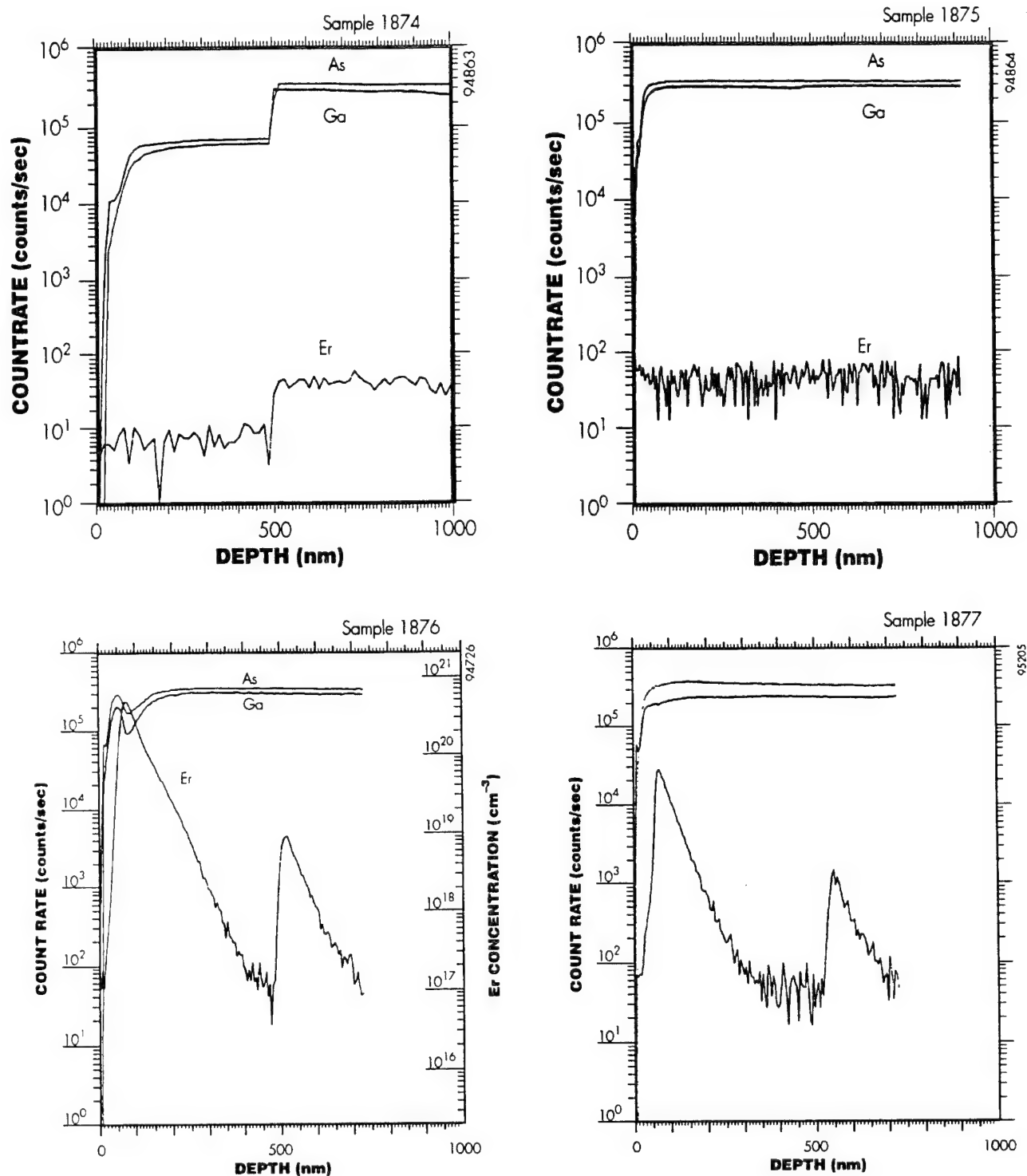
Figure 5 *SIMS of samples 1874, 1875, 1876, and 1877 (Table 2) demonstrating variation of erbium with process parameters. (Change in sputtering rate on sample 1874 changed signal levels.)*

10
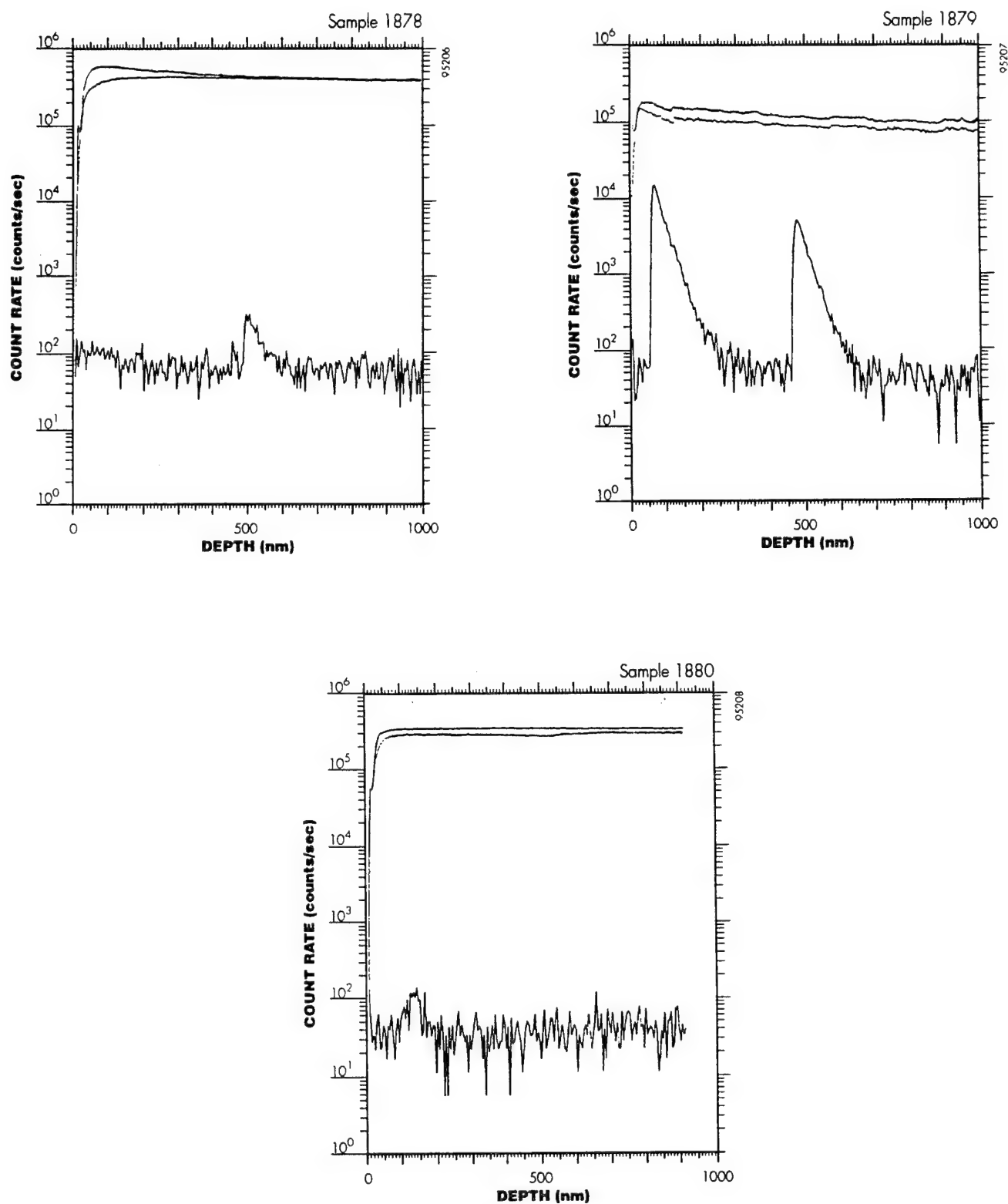
Figure 6   *SIMS of samples 1878, 1879, and 1880 demonstrating variation of erbium content with process variables (Table 2).*

11
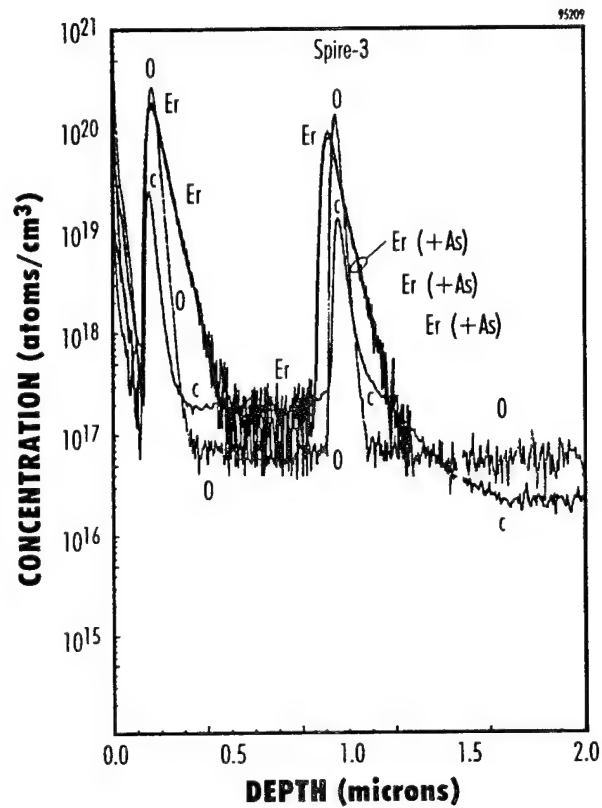
Figure 7 *SIMS data for sample 1879 showing erbium, carbon, and oxygen profiles. Increase in width of erbium peak relative to C and O implies rapid dopant diffusion.*
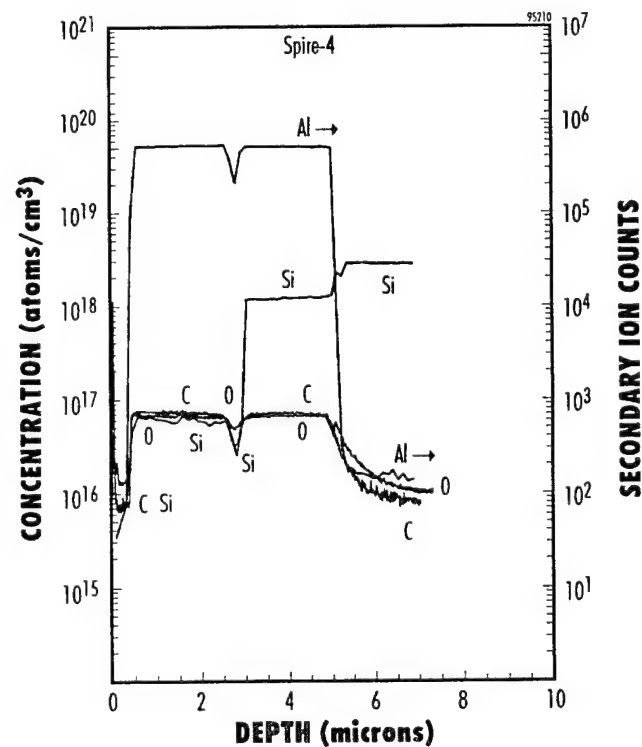
Figure 8 *SIMS data for good quantum-well laser wafer fabricated at Spire showing preferred carbon and oxygen levels.*
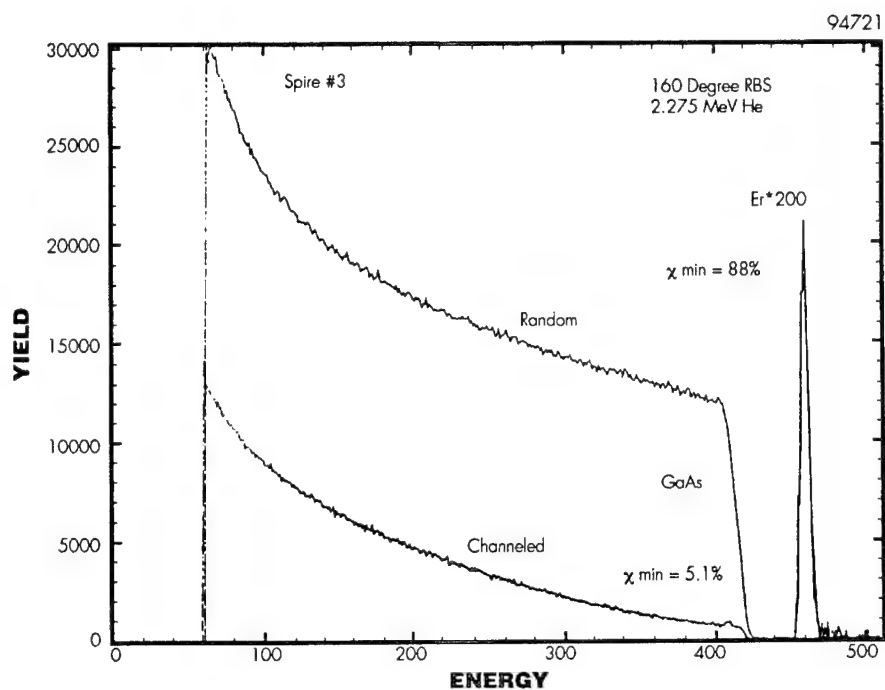
Figure 9   *Rutherford backscattering spectroscopy (RBS) data for sample 1879 showing erbium peak. This data was used to calibrate the erbium signal in SIMS data.*

Table 3   *Time-temperature profiles for GaAs and AlGaAs deposition.*

| Step # | GaAs (1941) | | AlGaAs (1942) | | Description of Deposition Step |
	Temp. (°C)	Time (sec)	Temp (°C)	Time (sec)	
1	100	10	100	10	purge and start arsine flow
2	650	600	720	600	heat up substrate, Er bypass flowing to reactor
3	650	15	720	15	increase arsine flow
4	650	120	720	120	deposit GaAs or AlGaAs buffer layer
5	650	120	720	120	deposit GaAs/AlGaAs with 100 sccm Er flow
6	650	120	720	120	deposit GaAs/AlGaAs with 200 sccm Er flow
7	650	120	720	120	deposit GaAs/AlGaAs with 400 sccm Er flow
8	650	600	720	600	deposit with Er (400 sccm) and arsine only
9	650	60	720	60	deposit capping GaAs or AlGaAs layer
10	100	900	100	900	cool down
11	100	10	100	10	turn off arsine flow and purge

These two samples were analyzed by SIMS and RBS as for sample 1879 etc. described above. Figure 10 shows the oxygen ion beam SIMS data for sample 1941 (GaAs), Figures 11 and 12 show the Cs$^+$ beam SIMS data for both samples, and Figure 13 gives the RBS data, and deduced concentration-depth plot for sample 1941.
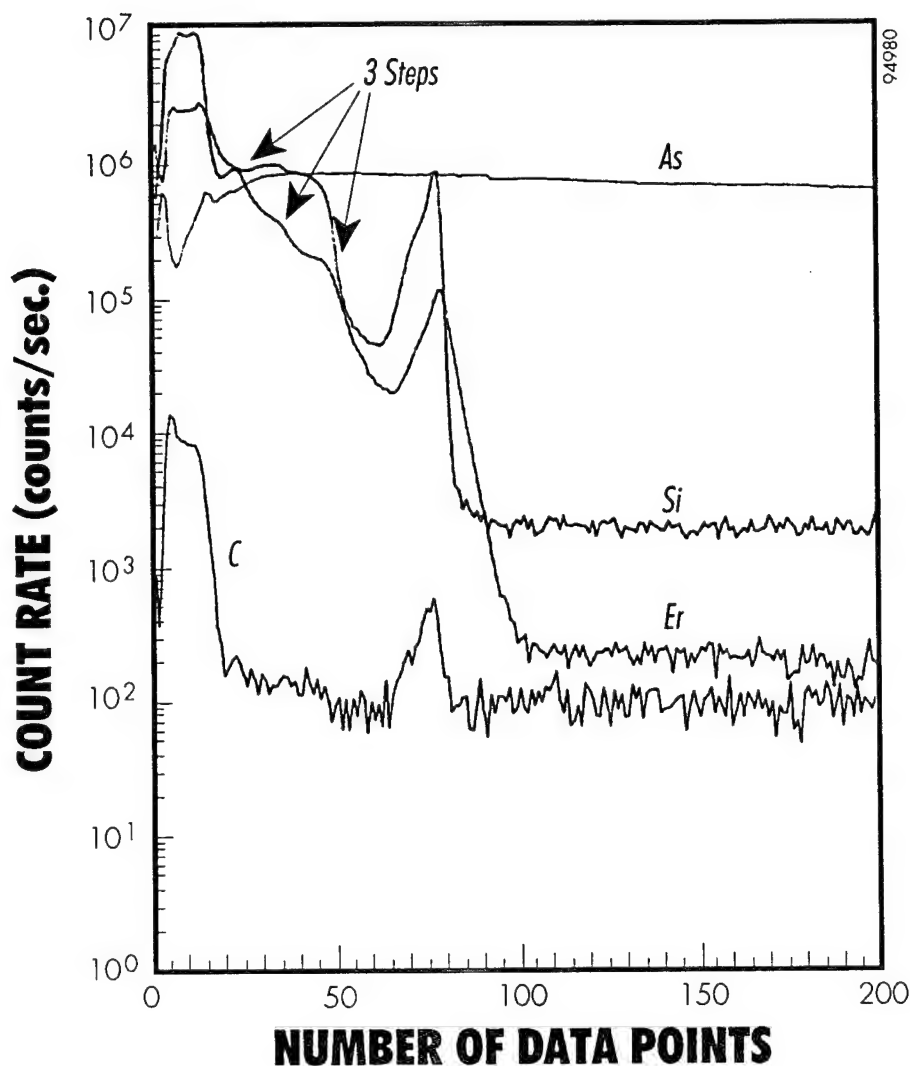
Figure 10   *SIMS data for sample 1941 with oxygen ion beam. Note that the three steps for the erbium concentration profile lie below the curve for the silicon concentration profile. The ratio of these two elements in NOT calibrated in this data.*

14
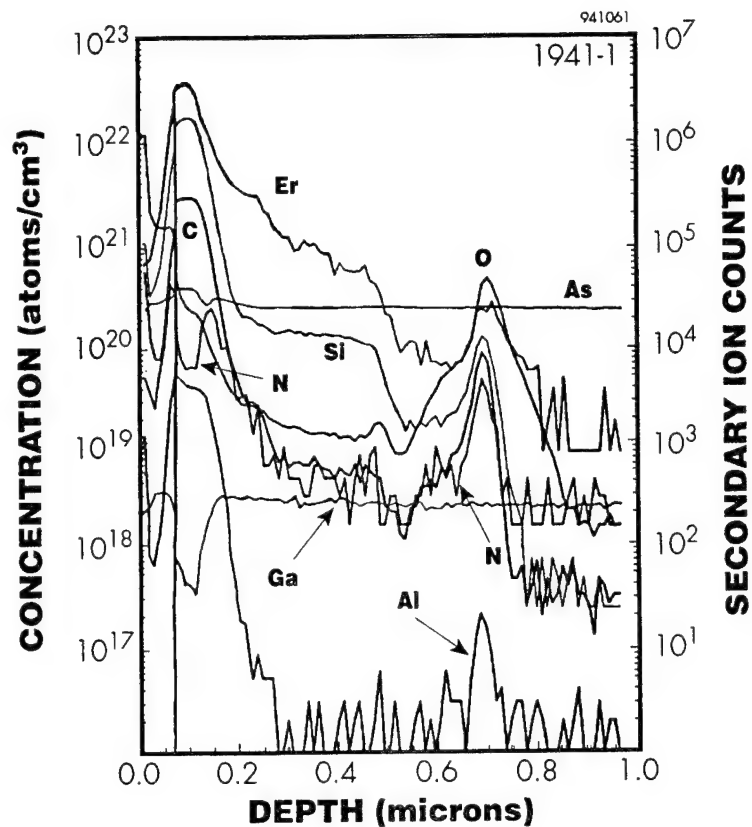
Figure 11 *SIMS data for sample 1941 with Cs ion beam.*
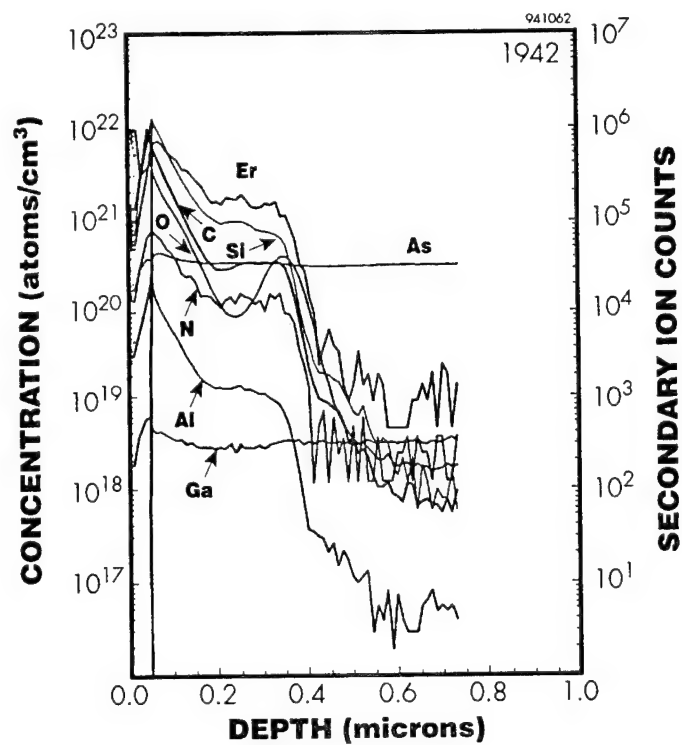
Figure 12 *SIMS data for sample 1942 with Cs ion beam.*

15

At the time these layers were deposited, there was no *a-priori* knowledge of the erbium concentration to expect in the film. Therefore, to assure that the instrumentation would detect some erbium, the last layer was deposited with the flow of gallium turned off. This created the very high erbium concentration (30 atomic %) layer which created the haze on the surface, and prevented RBS from acquiring ion-channeling data to determine the percent of erbium that was substitutional. The layers below the surface are more typical of the target composition. Figures 10 and 13, especially, show a stepped distribution of erbium in the deposited film below the major peak. These steps corresponded to the changes in carrier gas flow shown in Table 3. Thus, Spire demonstrated control of erbium concentration in the film. (The deep lying erbium peak deposited before the buffer layer was caused, as mentioned previously, by rapid purging of a dead spot in the carrier gas flow lines.

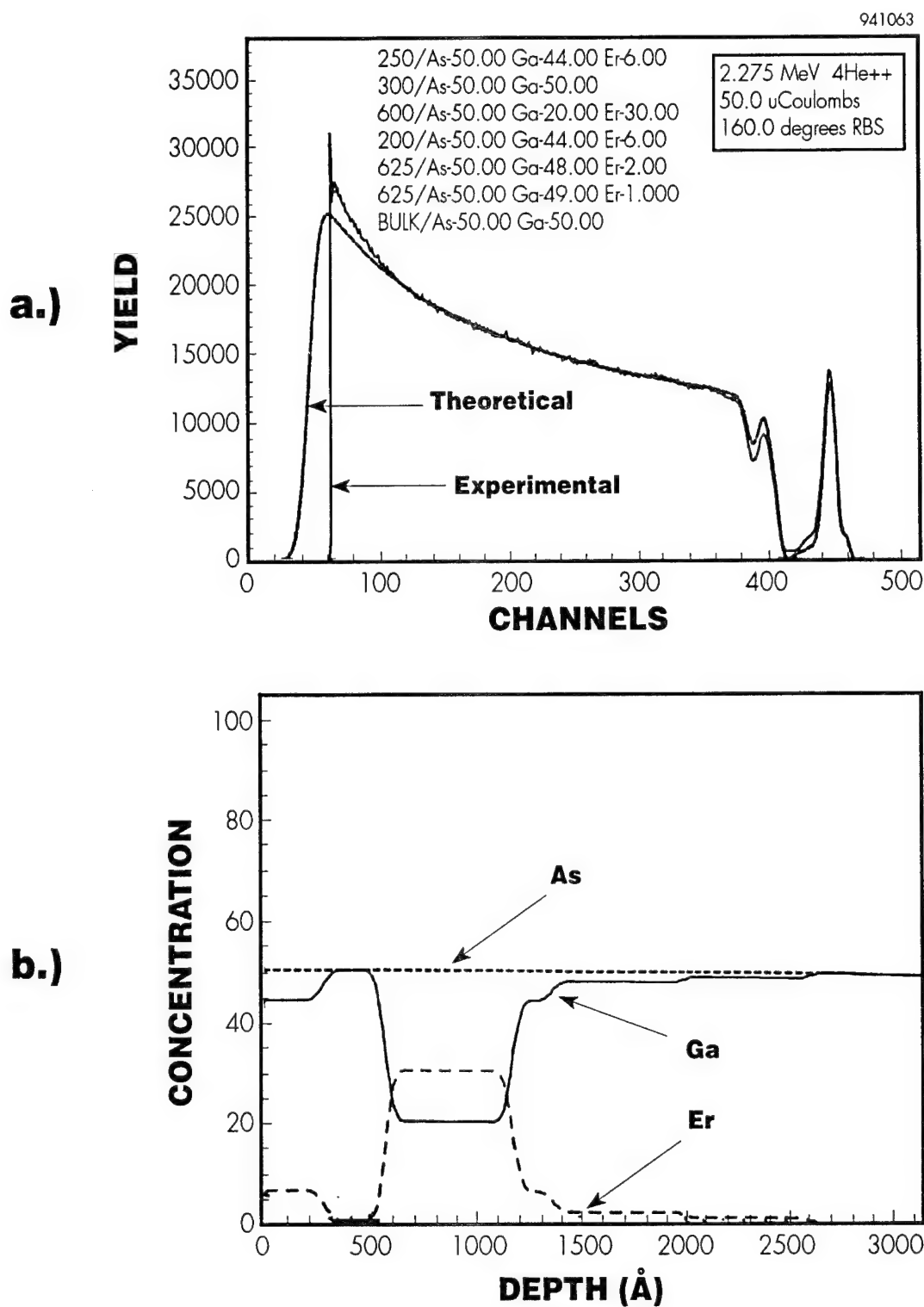The level of contaminants in the films in the region of 1 to 6 atomic percent erbium concentration was greater for the AlGaAs structure than for the GaAs structure. Figure 10 showed that the level of carbon stayed at background minimum detectivity (uncalibrated) for this region in GaAs, while Figure 11 showed that the carbon levels are about a factor of ten above the minimum detectable level (5×10^{18}/cc). In the AlGaAs structure the carbon levels were 4 to 5×10^{20}/cc. The oxygen concentration in Figure 11 had peaks at the surface and at the point of initial growth. Through the lower doped erbium layer the oxygen concentration was less than a factor of ten above the minimal detectable level at about 10^{19}/cc. The concentration of nitrogen in the GaAs sample was near the minimal detectable levels (sharp spikes are a single ion detected) and could be zero, while in the AlGaAs sample the concentration of nitrogen was over 10^{20}/cc. Detected levels of silicon followed the same pattern. In GaAs layers the silicon concentration was about 10^{20}/cc but almost 10^{21}/cc in AlGaAs layers.

This data was interpreted as a change in rate of chemical reactions with increasing temperature. The source for C, N, and Si in the film is the erbium precursor $Er\{N[Si(CH_3)_3]_2\}_3$. Residual leaks or source contaminants were the source for the oxygen. The AlGaAs layer was deposited at higher temperatures ($720°C$) than the GaAs layer ($650°C$). The erbium precursor decomposed faster at higher temperatures leaving behind copious amounts of silicon, nitrogen, and carbon. Doping of AlGaAs must be performed at lower temperatures when using erbium amides. The data implied that the level of contaminants of C, N, and Si seen in the GaAs could also be reduced at lower growth temperatures. Note that the growth temperatures used in this experiment were standard for deposition of laser structures at Spire.

When analysis of these two runs showed that erbium was incorporated into the III-V semiconductor crystal at high concentrations, proportional to the carrier flow through the erbium source, another set of deposition experiments was conducted with this erbium source to fabricate the deliverables for the first year of the program.

The deliverables were from run 2052 and 2052. Deposition steps for 2051 were identical to those in Table 3 above, lines 1, 2, 3, 5, 10 and 11. There was no buffer layer deposited, only one erbium layer (with constant carrier flow) and no capping layer. Heating and cooling cycles were as shown. For run 2052, the carrier flow of erbium was reduced to 50 sccm from the 100 sccm given in Table 3, step 5.

941063

a.)

250/As-50.00 Ga-44.00 Er-6.00
300/As-50.00 Ga-50.00
600/As-50.00 Ga-20.00 Er-30.00
200/As-50.00 Ga-44.00 Er-6.00
625/As-50.00 Ga-48.00 Er-2.00
625/As-50.00 Ga-49.00 Er-1.000
BULK/As-50.00 Ga-50.00

2.275 MeV 4He++
50.0 uCoulombs
160.0 degrees RBS

Theoretical

Experimental

b.)

As

Ga

Er

Figure 13   *RBS data (top) for sample 1941 and depth-concentration plot interpreted from data (bottom).*

17

The surface from run 2051 was very smooth, but a slight haze was seen for run 2052. Because of the haze, run 2053 was a repeat of run 2052 and also showed a slight haze. Run 2054 repeated the work a third time but at a lower growth temperature, only 600°C instead of 650. The haze factor was greater. Analyses showed that the haze was caused by excess erbium at the start of the growth cycle. During purging of the reactor, a pressure burst from a dead space in the feed lines caused a thin layer of nearly pure erbium source material to coat the substrate at low temperatures. This layer was converted to erbium arsenide during heating, and diffused into the substrate. Lattice mismatch with the semiconductor compound layer resulted in the haze on the wafer surface. The first run, with no erbium source material in the lines at the start of the purge cycle, had a smooth surface.

Photoluminescence spectra from samples 2051 through 2054 are shown in Figure 14. As the surface quality degraded with increasing number of runs (due to the initial, inadvertent doping layer) the signal strength decreased. Only samples from the first two runs were delivered to AFOSR. All samples were 2 inch diameter wafers. A separate small piece, typically a quarter wafer slice, was also included for each run so that Spire would have some separate material for our own characterization, as reported below, and could deliver the entire 2" wafer to the government.

Data for sample 2051 was verified separately by cathodoluminescence, shown in Figure 15. Additional detail at wavelengths just above 1.539nm was observed, but not explained at this time.

Data for erbium profiles and contamination were taken again by SIMS (Figure 16) using an oxygen ion beam. For sample 2051, grown first, before saturation of the erbium carrier line, there is no deep peak at the start of growth. The erbium concentration ramps upwards with deposition time as the carrier line became saturated with the source compound, increasing the concentration of erbium in the vapor phase at the delivery point to the reactor. For sample 2052, there is a peak at the start of deposition, again due to the purging cycle. Because the erbium line was exposed to the atmosphere between each run, the carrier line had to be saturated with the source for each run. The operator typically allowed 15 minutes for this saturation to run to completion, based upon results with III-V metalorganic compounds. The slowly increasing level of erbium in the film implies that the time required for saturation with erbium amides is greater. Note especially the low levels of carbon in the film, equal to background through the film and substrate, and the lower levels of silicon, calibrated to the substrate composition.

Sample film number 2051 was also analyzed by RBS (Figure 17) and by SIMS using a cesium ion beam (Figure 18). The erbium concentration, about 8×10^{18}/cc agreed closely with earlier results and previous calibrations. Because this sample had a smooth surface, the crystal structure was good and channeling analysis to determine the ratio of erbium that was substitutional in the host lattice was possible. The data indicated that about two-thirds of erbium present was on lattice sites and only one-third was interstitial. Comparison of the contamination levels to those found in sample 1879 (Figure 11), showed that the silicon and nitrogen concentrations were about a factor of ten lower while the oxygen and carbon concentrations were about the same. Deposition temperatures for sample 1879 and 2051 were identical at 650°C.
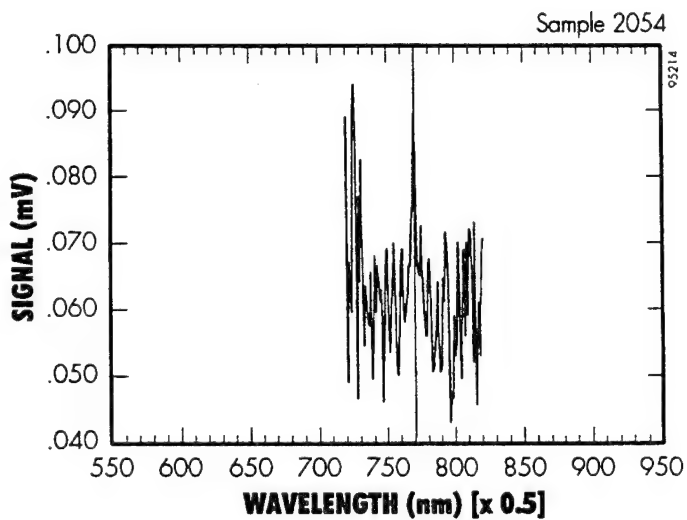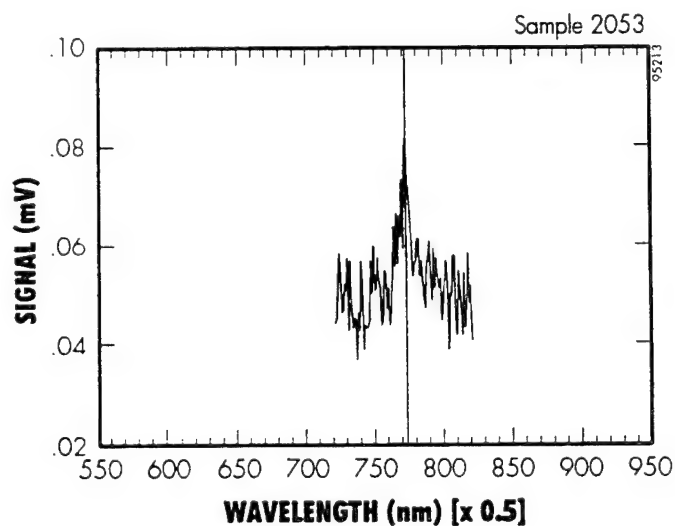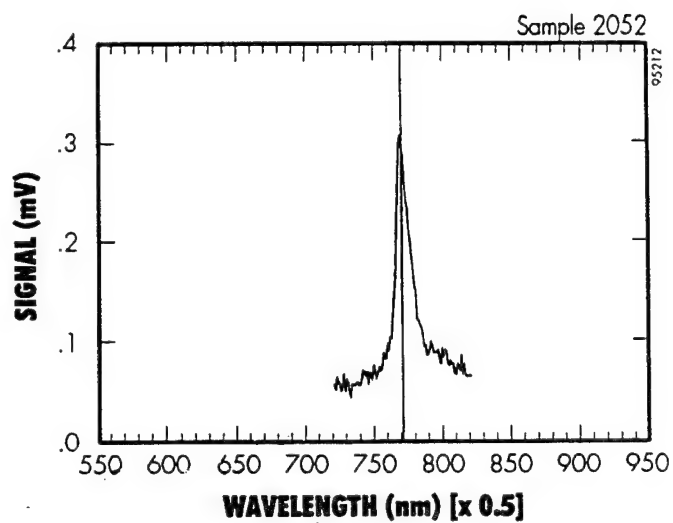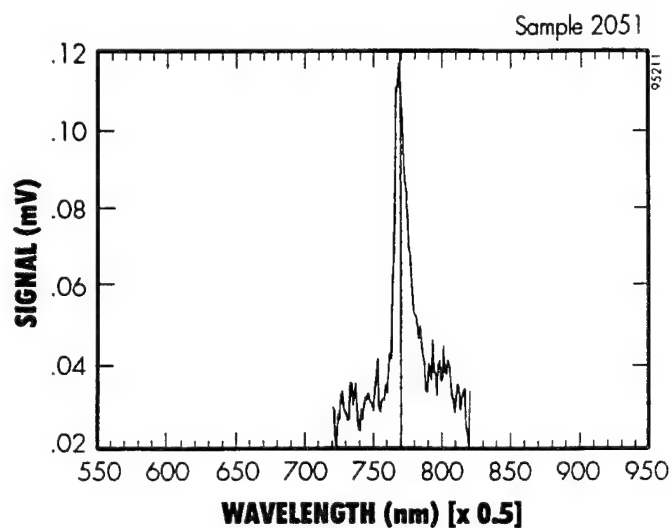
Figure 14 *Photoluminescence data from samples 2051, 2052, 2053, and 2054 measured at 77K showing clear, sharp peak at about 1538 nm. Note that the signal strength was reduced as the level of surface haze increased.*

19
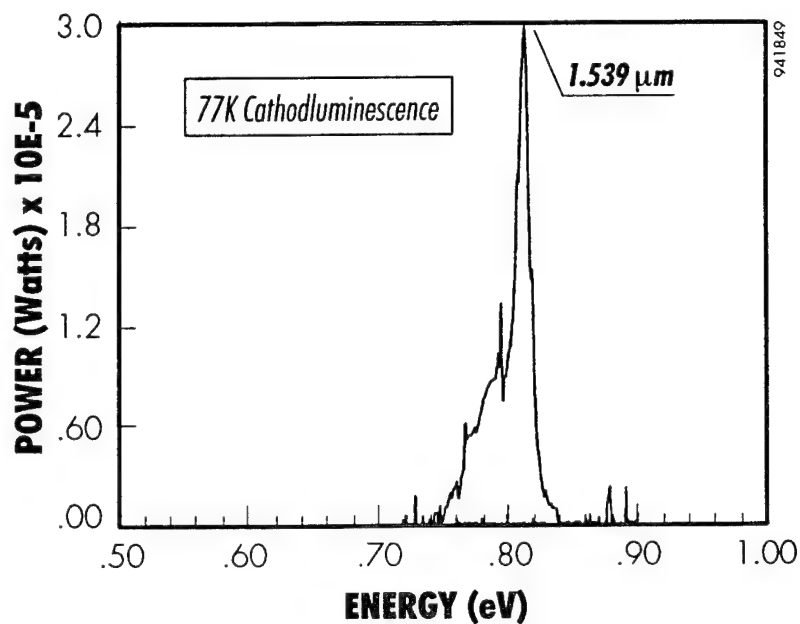
Figure 15 *Cathode-luminescence spectra for sample 2051 at 77K.*
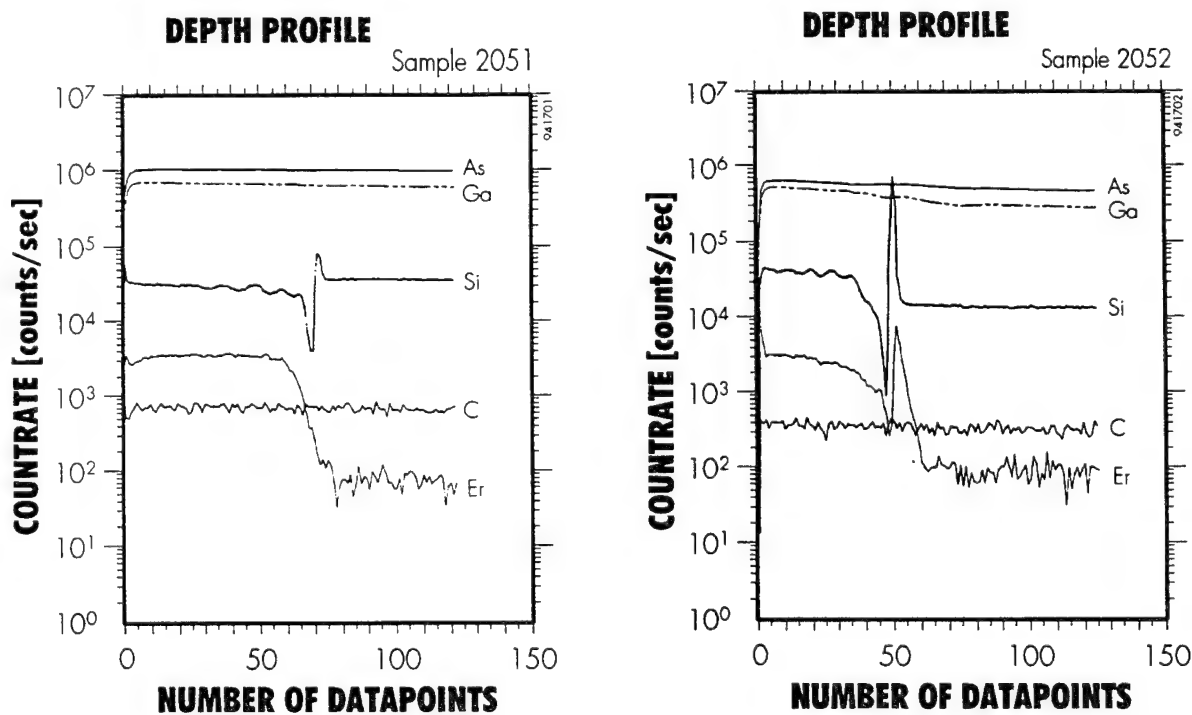
Figure 16 *SIMS data using an oxygen ion beam for samples 2051 and 2052, delivered to AFOSR. Nominal erbium concentration from calibration in Figure 15 is between 6 and 7 x 10^{18}/cc.*
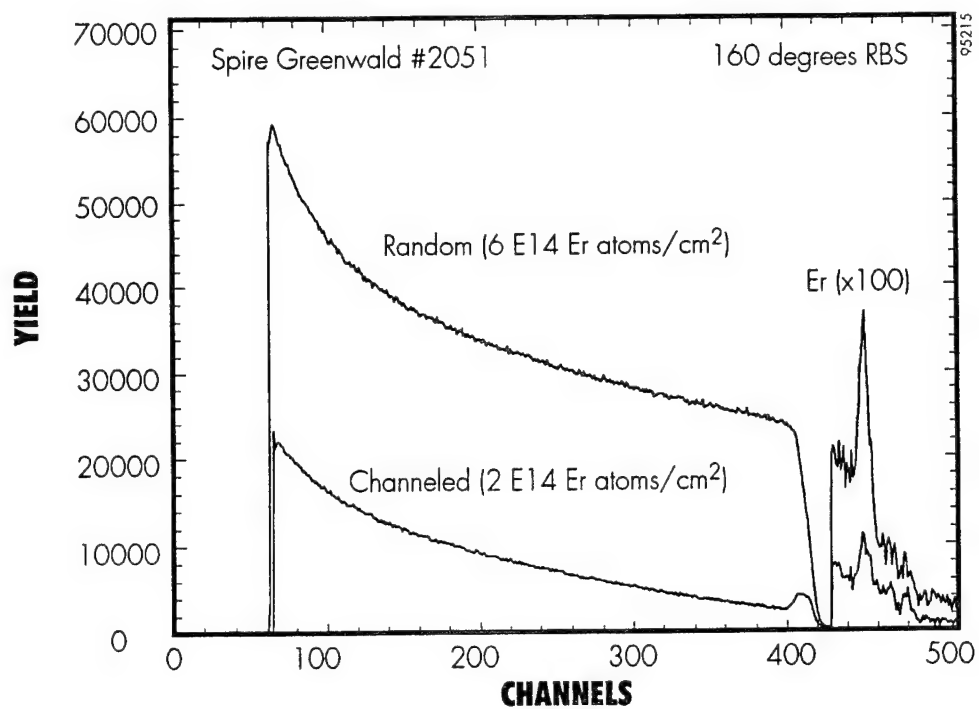
Figure 17 *RBS data for sample 2051 showing random and channeling spectra, indicating 2/3 of the erbium dopant was substitutional.*
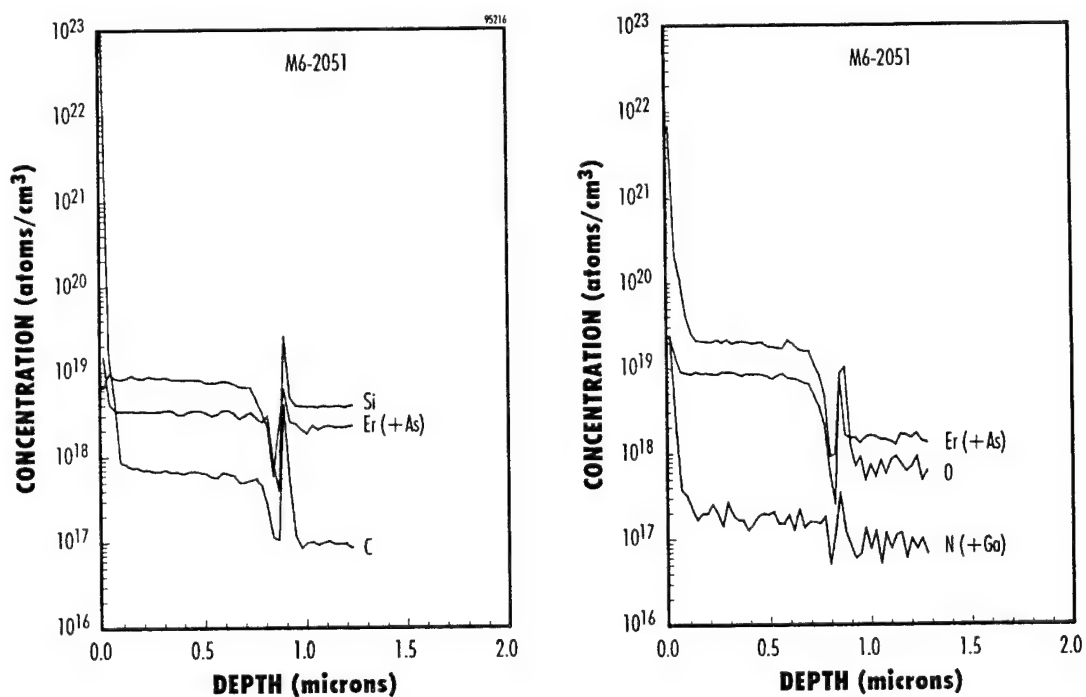
Figure 18 *SIMS data of sample 2051, taken with a cesium ion beam showing oxygen and nitrogen levels (left) and silicon carbon levels (right).*

2.3.3 Tris-triethyldisilylamido-erbium

The objective of this set of tests was to determine if use of an alternate erbium source would reduce the amount of silicon remaining in the GaAs deposited layer when doped with erbium using disilylamines. Incorporation of silicon as a dopant in these films from the erbium source is a thermal driven chemical reaction and altering the starting point can control the results.

Nominally, it requires more energy to separate the ethyl bond from the silicon atom than the methyl bond, so that the organic radical N - Si - Et_2 (where Et is CH_2CH_3) would be expected to have slightly greater stability than the methyl substituted source radical. As the erbium source decomposes when adsorbed on the substrate surface, this greater stability of the silicon atom bonds promote formation of $NHSi(Et)_2$. The radical containing Si combines with the free hydrogen atoms released from arsine decomposition, instead of breaking into C_2H_6 and ammonia. This should reduces the amount of silicon in the deposited film at constant temperature relative to the methyl source.

Thermal gravimetric analysis of this source was not available at the time the set of experiments was to be performed. Without reliably knowing the decomposition temperature, or the vaporization curve, the experiments tested the operating temperature of the source as the key variable. All other parameters were kept as in run 2051, the deliverable. Source temperature were slowly increased from 110 to 160°C in 10 degree steps. Photoluminescence measurements were used as a prime indicator of erbium doping. No signals were seen and the experiments were discontinued.

2.3.4 T-butyltrimethylsilylamido-erbium

The chemical, $Er\{N\ (^tBu)\ SiH(CH_3)_2\}_3$, was synthesized according to Section 2.1.3. MOCVD parameters for growth of epitaxial GaAs films were (a) source temperature of 160°C, carrier gas flow of 100 sccm, source pressure of 300 torr, gallium carrier flow of 8 sccm, III/V ratio of 150, reactor pressure of 75 torr, and substrate temperature of 600°C. SIMS data for this erbium doped film are shown in Figure 19. Prior data was used for calibration.

SIMS data in Figure 19 shows that the silicon concentration follows the erbium concentration profile, which would be expected if both species came from the same source. The dopant concentration peaks at the surface for both samples. This is not due to diffusion. The long gas line between the source and the growth chamber requires some minimum time for saturation. As this film was deposited with reduced time allowed for saturation, the concentration of erbium in the film increases with deposition time and is greater near the end of the run, at the surface. Saturation times were reduced for this experiment because we had only ten grams of this source material (compared to 100 grams of the $Er\{N[Si(CH_3)_3]_2\}_3$ source now available from a commercial supplier). The erbium concentration did approach 10^{19} cm^{-3} at the surface, but the PL response was too weak to be detected. The SIMS data also gives the ratio of silicon to erbium in these films as more than a factor of ten greater than the Si:Er for films deposited with the methyl-silyl-amide at the same temperature (see below). Because excess silicon is undesirable, we stopped experiments this material.

22
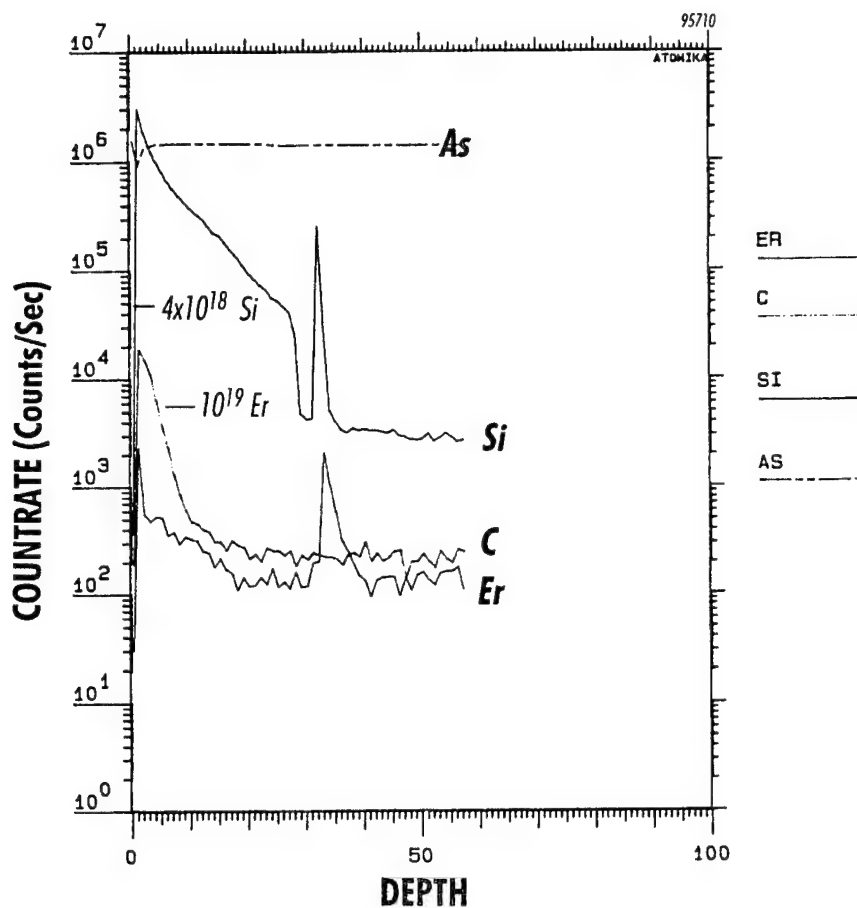
Figure 19 *SIMS data for sample 2233, GaAs:Er deposited from Er{N(t'Bu)SiH(CH₃)₃)₂}₃ showing increase in erbium concentration with growth time, and large silicon concentration.*

In the figure, the following labels appear: COUNTRATE (Counts/Sec) on the vertical axis, DEPTH on the horizontal axis, with curves labeled As, Si, C, Er, and annotations "4x10^18 Si" and "10^19 Er", legend entries ER, C, SI, AS, and "95710 ATOMIKA".

2.3.5 Conclusions from Initial Growth Experiments

Spire successfully doped gallium-arsenide and aluminum-gallium-arsenide with erbium using disilyl-amide erbium metalorganic compounds during MOCVD growth of epitaxial layers. The erbium concentration could be varied up to 30 atomic percent, but the surface of the film remains smooth only up to a doping level of about 10^{19}/cc. The erbium concentration in the delivered samples was 8 x 10^{18}/cc. Of this total, about two-thirds or over 5 x 10^{18}/cc was substitutional in the GaAs lattice.

Contamination levels were reduced in the delivered samples compared to carbon doping seen with the use of cyclopentadienyl derivatives. Typical carbon concentrations were below 10^{18}/cc. Typical nitrogen concentrations were below the minimum detectable level for this technique for growth at 650°C. Typical silicon concentrations were below 5 x 10^{18}/cc and less than that in the substrate. Silicon incorporation varied with growth temperature, a rough plot of this variation is shown in Figure 20 below. The diffusion rate of erbium was greater than that of carbon or silicon in GaAs as determined from broadening of the curves. Estimates for the diffusion coefficient D at 650°C were 1 x 10^{-15}cm^2/sec.

23
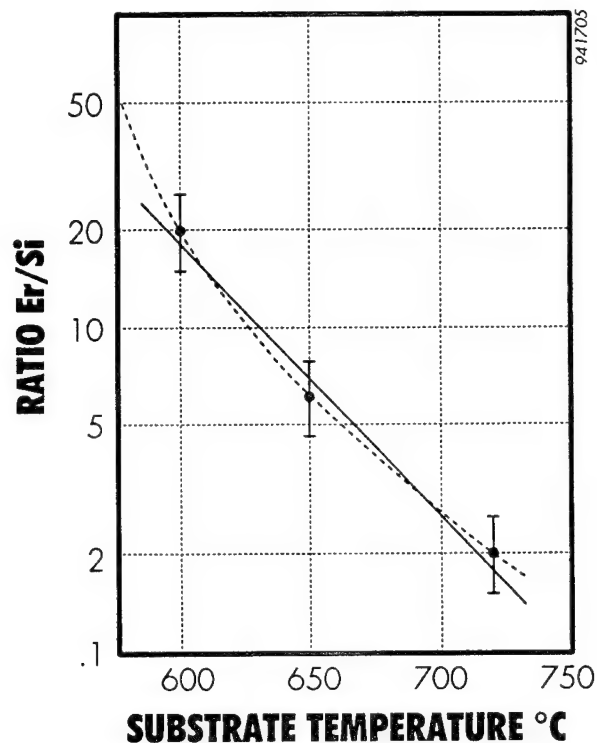
Figure 20 *Preliminary determination of silicon doping levels as a function of growth temperature for trimethyl-disilylamido-erbium.*

Photo-luminescence (excited by a 488 nm argon ion laser) and cathode-luminesce spectra of erbium at 77 K showed sharp peaks at the 1539 nm wavelength.

2.4 Design and Fabrication of Er-doped Quantum Well Diode-laser

2.4.1 Design Study

Our initially proposed design for an erbium-ion laser assumed that the erbium ions could be pumped into the high energy state by optical absorption of the light from the normal laser-diode emittance. (Contrary data in Section 2.6 was only available near the end of the program.) Erbium glass lasers are typically pumped at 980 nm, corresponding to a broad absorption band. Use of this band implies that small variations of pump wavelength with temperature from the semiconducting part of the system built by Spire will still effectively pump the erbium ions, so that emission at 1538 nm will not change.

This task then started with the design of a 980 nm, SINCH-SQW laser shown in Figure 21. Experiments were conducted to calibrate the MOCVD reactor for exact composition of the different layers required, and the structure was grown on five wafers. Photoluminescence (PL) was used to estimate the output wavelength of the structure when fabrication is complete. One wafer was judged to be out-of-spec (yield loss), and laser arrays were fabricated from the other four wafers.

Results of electrical and optical tests are summarized in Table 4. The lasers operated very well with emission within the design limits. This will now be offered as a product in Spire's line of diode lasers, as wafers, as laser bar arrays, and as mounted laser bar arrays for pumping erbium-doped solid state lasers.

24
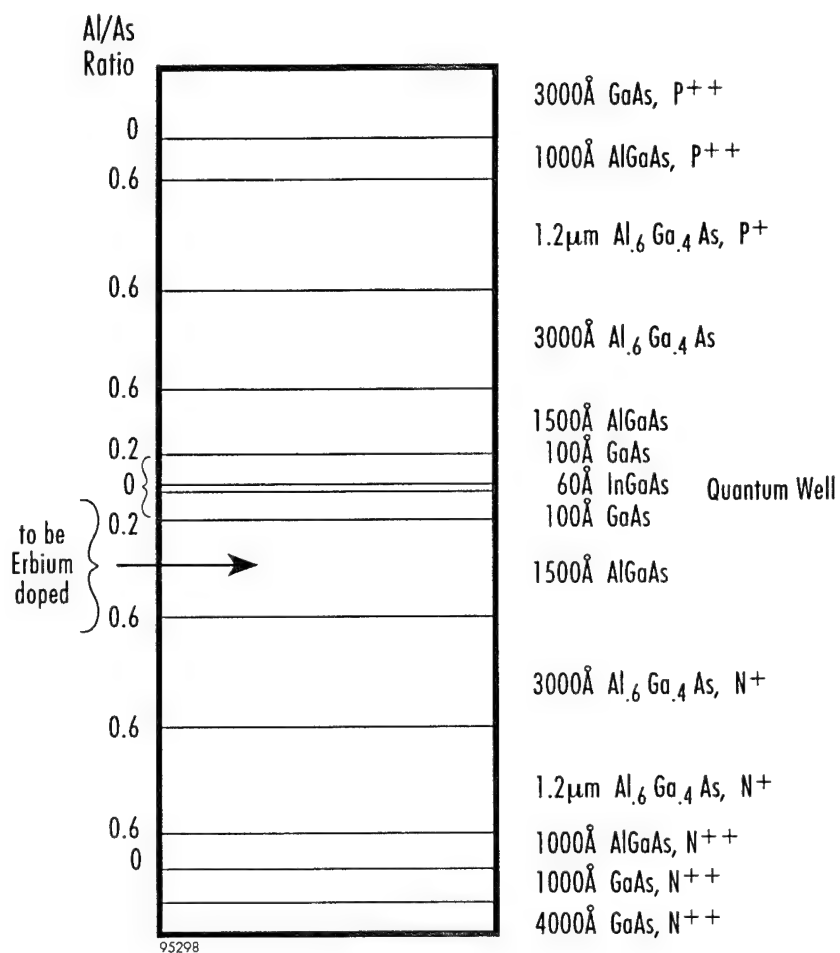
Figure 21   *Design of "pump" laser at 980 nm.*

Table 4   *Summary of parameters for 970 nm pump lasers.*

Package I.D.	Threshold current A	Slope Efficiency	Peak Power (W)	Resistance (mΩ)	wavelength (nm)	FWHM (nm)
171	11.1	.903	44	7.6	970.2	2.6
172	7.9	.887	46	7.3	972.2	2.4
173	8.9	.879	45	6.7	971.4	2.6
174	11.7	.840	41	7.9	970.4	2.5
typical	8	1	45	4-8	800±2	2.5

MOCVD Run number M4-3705, Process lot 5822

25

The AlGaAs waveguide regions which carry the light must be undoped to reduce free carrier absorption in the laser design of Figure 21. Our earlier results showed that the amount of silicon in the erbium doped film increases with an increase in deposition temperature. Because CVD films show an increase in oxygen content of AlGaAs films deposited at low temperatures it is not possible to have low silicon content and low oxygen content in the same AlGaAs film. Therefore, a change in laser design was mandated by experimental results.

It was decided that the AlGaAs layer in the waveguide could be simply replaced with GaAs where we do not have as severe a problem with oxygen incorporation. This is possible because the difference in absorption between GaAs and AlGaAs is not significant at this long wavelength. This led to the structure shown in Figure 22a. Further calculations, Figure 23, showed that the light at 1.54 μm would overlap the region near the waveguide edge where the doping level was high. This led to another change in laser design, Figure 22b, reducing the doping level of the cladding layer adjacent to the waveguide region. Figure 22b thus became the new target for erbium doped laser fabrication.

a)

| Thickness	Material	Doping
3000	GaAs	$\geq 10^{19}$ Zn
1000	Al$_{.6}$Ga$_{.4}$As	$\geq 8 \times 10^{18}$ Zn
12000	Al$_{.6}$Ga$_{.4}$As	$\geq 10^{18}$ Zn
200	GaAs	
1500	GaAs	10^{19} Er
100Å	GaAs	
60Å	InAlGaAs	
100Å	GaAs	
1500	GaAs	10^{19} Er
200	GaAs	
3000	Al$_{.6}$Ga$_{.4}$As	$\geq 10^{18}$ Si
12000	Al$_{.6}$Ga$_{.4}$As	$\geq 10^{18}$ Si
4000	GaAs	Buffer
	GaAs	N+

Substrate
95730

b)

Thickness	Material	Doping
3000	GaAs	$\geq 10^{19}$ Zn
10000	Al$_{.6}$Ga$_{.4}$As	$\geq 5 \times 10^{18}$ Zn
3000	Al$_{.6}$Ga$_{.4}$As	$\geq 10^{17}$ Zn
200	GaAs	
1500	GaAs	10^{19} Er
100Å	GaAs	
60Å	InAlGaAs	
100Å	GaAs	
1500	GaAs	10^{19} Er
200	GaAs	
3000	Al$_{.6}$Ga$_{.4}$As	$\geq 10^{17}$ Si
12000	Al$_{.6}$Ga$_{.4}$As	$\geq 5 \times 10^{18}$ Si
5000	GaAs	Buffer

Substrate
95729

Figure 22   *Modified structure for 970 nm laser for erbium incorporation in GaAs layers. (a) Left side with original modification, run 2248; (b) right side with reduced doping adjacent to waveguide region.*

26
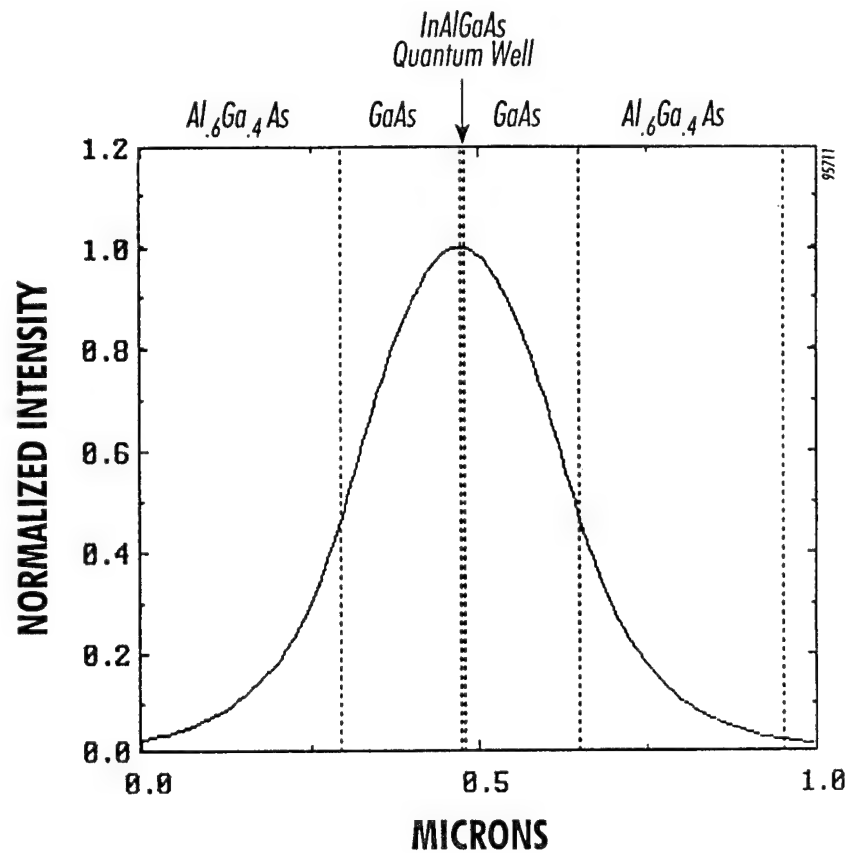
Figure 23   *Calculated containment of electromagnetic fields within waveguide region of laser in Figure 22a at 1540 nm showing spreading into doped cladding layers.*

Table 5   *Deposition parameters for erbium-doped films.*

Sample ID	Deposition Temp. °C	Source Press.	Buffer Layers	Common Parameters
2246	570	160	yes	Source = $Er\{N[Si(CH_3)_3]_2\}_3$
2247	530	250	yes	Source T = 160, flow = 200 sccm Reactor P = 75
2251	500	250	yes	Ga flow =2 sccm, V/III ratio = 100 Er deposition 3600 sec.
2252	600	250	yes	
2253	650	250	yes	GaAs buffer at 650, undoped, 250 sec
2254	550	250	yes	Ga flow at 8 sccm AlGaAs buffer at 650, 40%, undoped,
2256	500	250	no	1,000 sec.
2259	550	250	no	

27

All films were deposited with an AlGaAs buffer layer separating the GaAs:Er from the GaAs substrate so that measurement of the optical reflectance as a function of wavelength could be used to determine the deposited layer thickness. At least one piece of semi-insulating GaAs substrate material was included in each run for Hall characterization of the mobility and carrier concentration of the combined buffer and Erbium doped layers. At least one piece of N-type doped material was also used as a substrate so that the carrier concentration could also be measured by a POLARON™. A second piece of the N-type substrate sample for each case was forwarded for separate characterization of Er, As, Ga, O, C, N, and Si concentration by SIMS (secondary ion mass spectroscopy). Photoluminescence (PL) measurements at 77K (and some at 300 K) were made at Spire. The results are summarized in Tables 6 and 7. Note that Hall measurements for very high resistivity material, indicated by a question mark in Table 7, are not reliable.

Table 6   *Measured composition of erbium doped GaAs layers.*

Sample ID	Thickness (μm)	Er (10^{19}/cm^3)	Si (10^{18}/cm^3)	O (10^{19}/cm^3)	C (10^{17}/cm^3)
2246	0.41	?	7.0	0.5	6
2247	0.52	?	1.7	1.0	8
2251	1.12*	3.0	2.0	3.0	10
2252	0.59	2.0	8.0	2.0	10
2253	0.61	2.0	15	2.3	7
2254	0.54	1.3	3.0	1.0	10

In all samples, nitrogen was below minimum detection levels.
Thickness by fitting optical reflectivity data.
* Poor fit for this data point.

Table 7   *Electrical properties for erbium doped GaAs layers.*

Sample ID	77K peak PL signal	Polaron carrier conc.	N (Hall)	μ (Hall)	Resistivity (ohm-cm)
2246	0.3	$2 - 4 \times 10^{18}$	--	--	--
2247	0.5	depleted	6.7×10^{15}	2227	0.42
2251	.25	depleted	?	?	?
2252	.25	depleted	?	?	6800
2253	.15	$4-10 \times 10^{18}$	2.9×10^{18}	707	0.0031
2254	1.0	depleted	?	?	16,000
2256	0.27	depleted	?	?	133-321
2259	1.3		5.8×10^{12} ?	1234 ?	868

Film thickness was measured by analyzing optical reflectance data in the visible to near infrared for an erbium doped GaAs layer on top of an AlGaAs layer. Data was fitted using textbook values for the index of refraction. For sample 2251, however, the computer algorithm did not converge on an acceptable fit. Thicknesses deduced from SIMS measurements for these samples were not accurate as the sputtering rate for GaAs and AlGaAs differs by as much as much as 30%. Sample film thickness divided by the deposition time gives the growth rate.

One goal in the design of these experiments was to increase the erbium concentration from that seen in samples delivered to AFOSR (2051 and 2052). This could be accomplished by increasing the ration of erbium to gallium in the gas stream injected into the reactor. Because the relative concentration of erbium vapor could not be increased (i.e. parameters for a given source and mechanical arrangement were set to upper limits) we lowered the flow of gallium into the reactor. Reducing the gallium flow reduced the growth rate, but the final erbium concentration was about the same. There is some indication that erbium concentration increased with decreasing growth rate and temperature (Figure 24); however, there is too much scatter in data for firm conclusions.

The variation of silicon concentration in these films showed a straight forward variation with temperature (Figure 25) indicating an activation energy of about 1.5 eV. This can be interpreted as the energy required for breaking the silicon-nitrogen or silicon-methyl bonds. At lower temperatures, and especially in the presence of single hydrogen atoms moving across the substrate surface from the decomposition of arsine, hydrogen attachment to the nitrogen after removal of erbium allows evaporation of the volatile amino complex from the surface. At higher temperatures, the silicon bonds break too fast for evaporation of the entire radical. Data in Table 6 indicate little or no temperature variation for carbon, nitrogen, or oxygen content in the film.
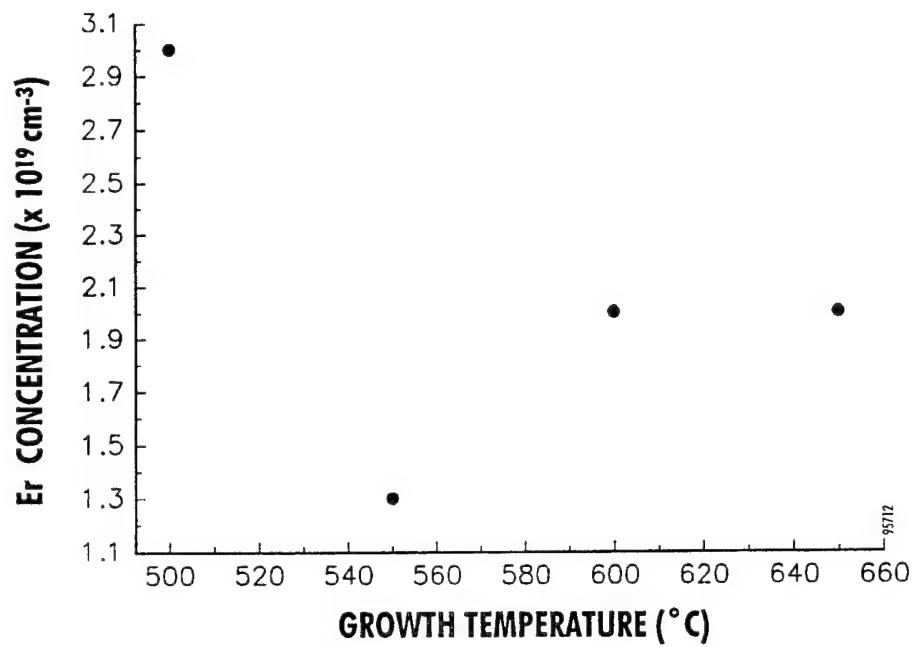
Figure 24   *Erbium concentration in GaAs as a function of deposition temperature.*
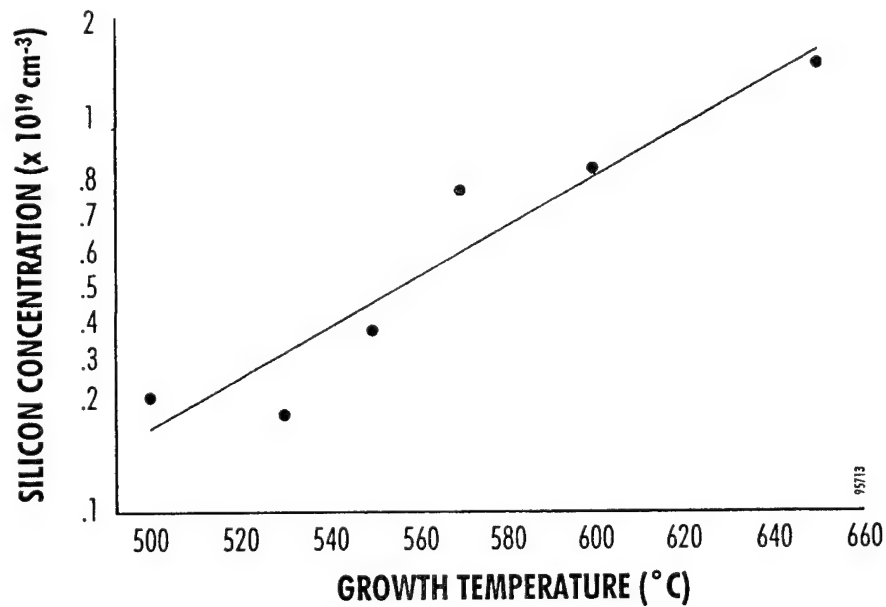

Figure 25   *Silicon concentration in GaAs films doped with erbium-amides as a function of deposition temperature.*

A sample photoluminescence (PL) signal from this group of films is shown in Figure 26. Table 7 shows some increase in the PL signal as the growth temperature is reduced. We cannot tell at this time whether this increase is due to an increase in the erbium concentration, a decrease in the silicon concentration, a possible increase in the oxygen concentration, or a structural variation. The peak wavelength of the PL signal for all samples fabricated during this reporting period was 1544±1 nm. This compares to a peak wavelength of 1540±2 nm for all samples fabricated in the group that was forwarded to AFOSR as deliverables. Offset from 1538 nm may be due to calibration shift.
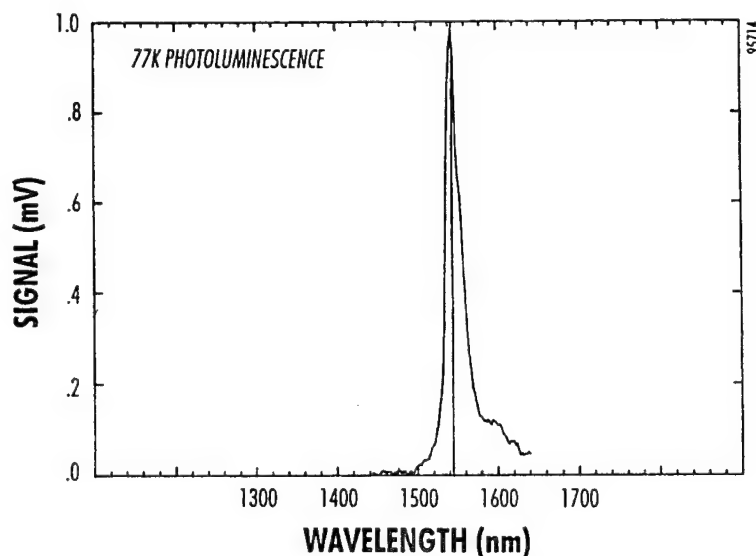

Figure 26   *Photoluminescence spectra from sample 2254.*

Photoluminescence (PL) data was also gathered from erbium doped laser structures. Sample 2248 had the structure depicted in Figure 22a, and sample 2249 has the identical structure, except that there was no erbium doping. Sample 2258 had the structure depicted in Figure 22b. Photoluminescence data from 2249 without erbium showed the expected strong peak from recombination at the quantum well at about 970nm (Figure 27). Sample 2248, with erbium, had no peak at 970 nm but did have PL emission at 1544 nm at 77K and a weaker signal at 300K (Figure 28). PL emission from sample 2258 was similar to that of sample 2248.

SIMS data for these structures are shown in Figures 29 and 30 for Cs^+ ion beam bombardment. The erbium signal was not separable from interferences for this apparatus. The quantum well is clearly viable as the center of a symmetric AlGaAs/GaAs structure. Erbium was added to the region outside of the quantum well (see Figures 22a and 22b). Silicon doping associated with this erbium source can be seen adjacent to the quantum well.

Why is the 970 nm emission absent from the erbium doped structure? One possibility is that the silicon associated with the erbium dopant moved the center of the diode junction away from the quantum well. However, all of the layers normally near the quantum well are slightly p- or n-type so that the center of the junction is never exactly at the quantum well. In this case, without erbium doping, the material has high mobility so that recombination at the quantum well is very likely. With erbium doping, the mobility is reduced so that recombination at the quantum well may not be likely.

31
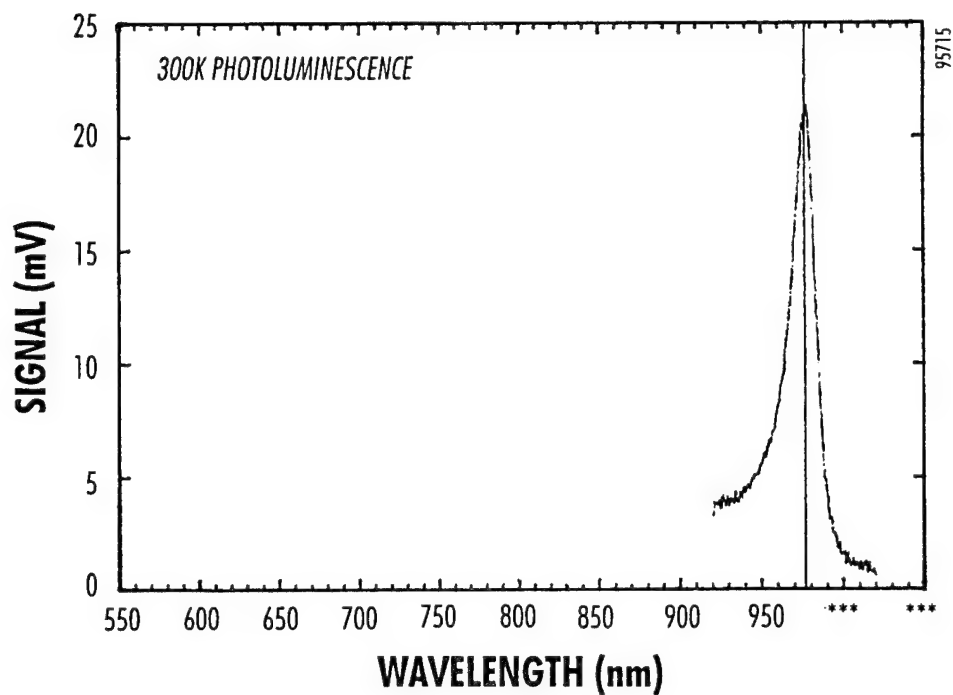
Figure 27   *PL spectra from sample 2249, a laser structure without erbium doping designed to emit at 970 nm.*
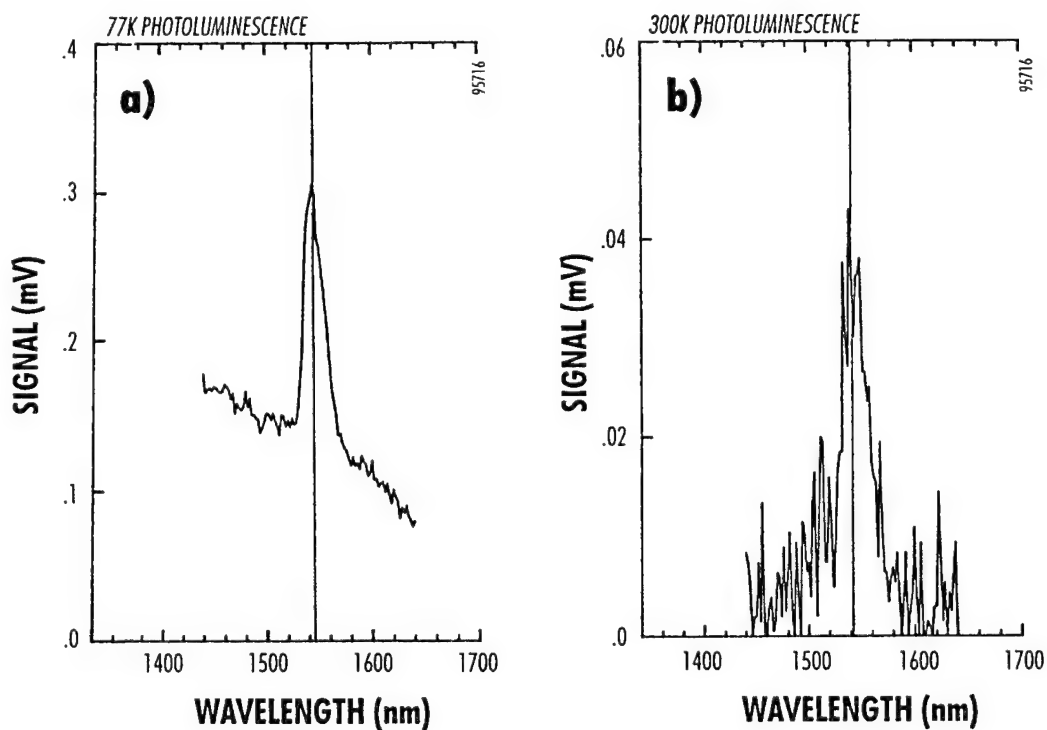
Figure 28   *PL emission form erbium doped laser structure (Figure 22) at 77K and 300K.*
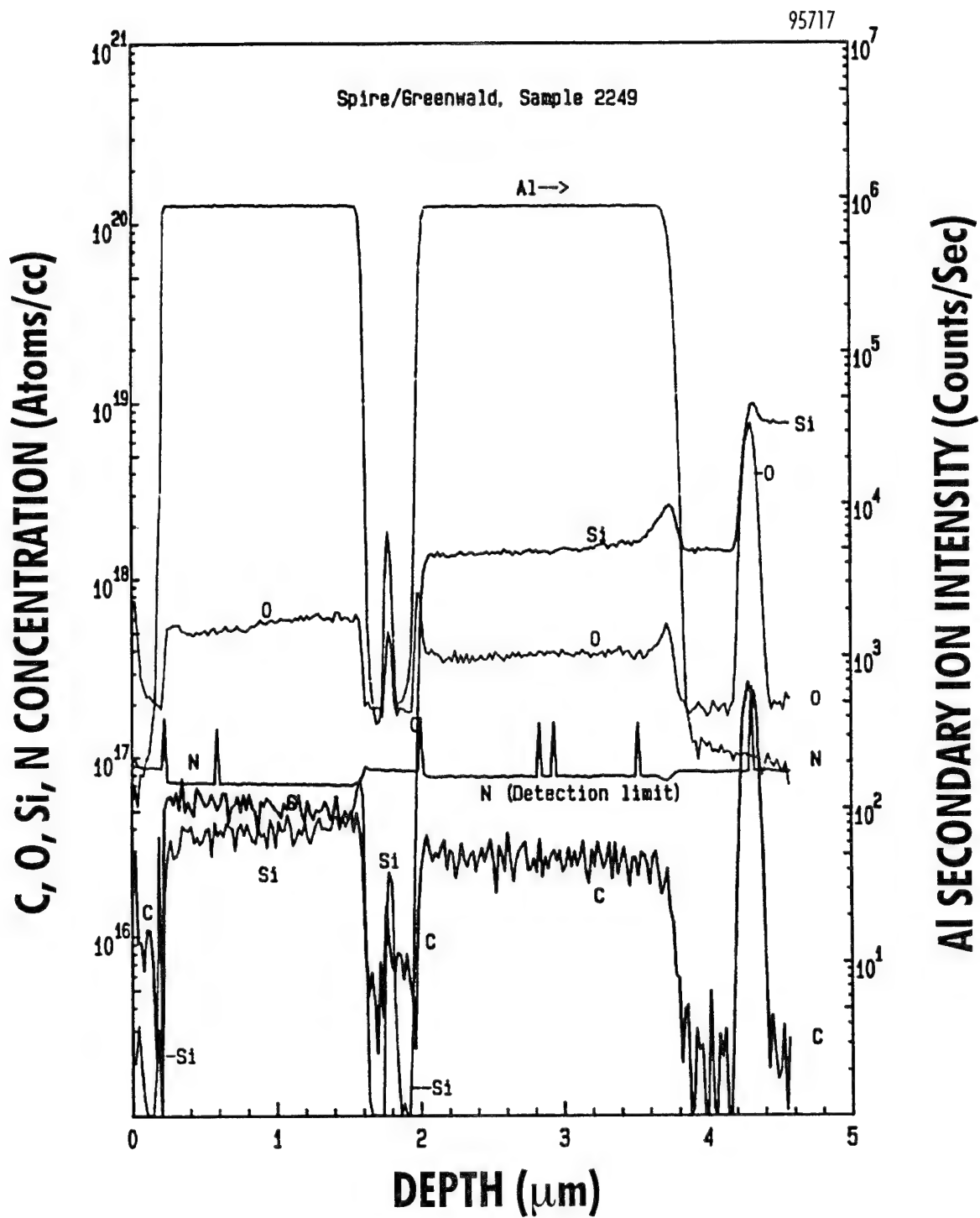
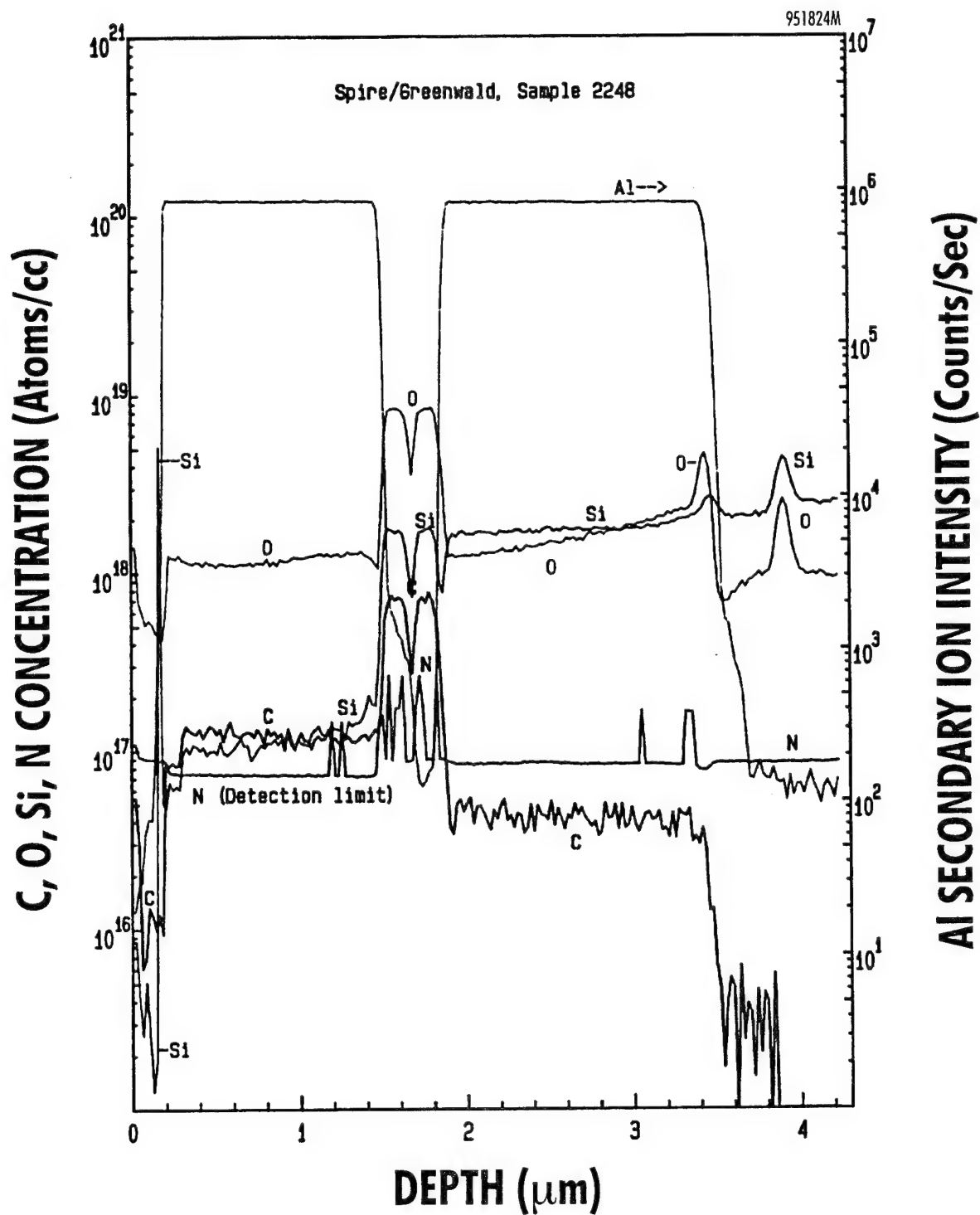**Figure 29** *SIMS data for laser structure with erbium.*

Figure 30 *SIMS data for laser structure without erbium.*

34

Figure 31 shows preliminary data on the minority carrier lifetime of Spire's erbium doped material, courtesy of the National Renewable Energy Laboratory (NREL). Data for an non-passivated structure such as an erbium doped GaAs layer directly on the surface should show high recombination due to surface effects. The laser structure is passivated but still shows very short lifetime effects, less than 100 ps. If erbium is a minority lifetime killer, then it must be removed from the lasing region of the device and the structure proposed in Figure 1 is more appropriate. The very recent publication by Seth supports the lifetime killer assumption.[15]
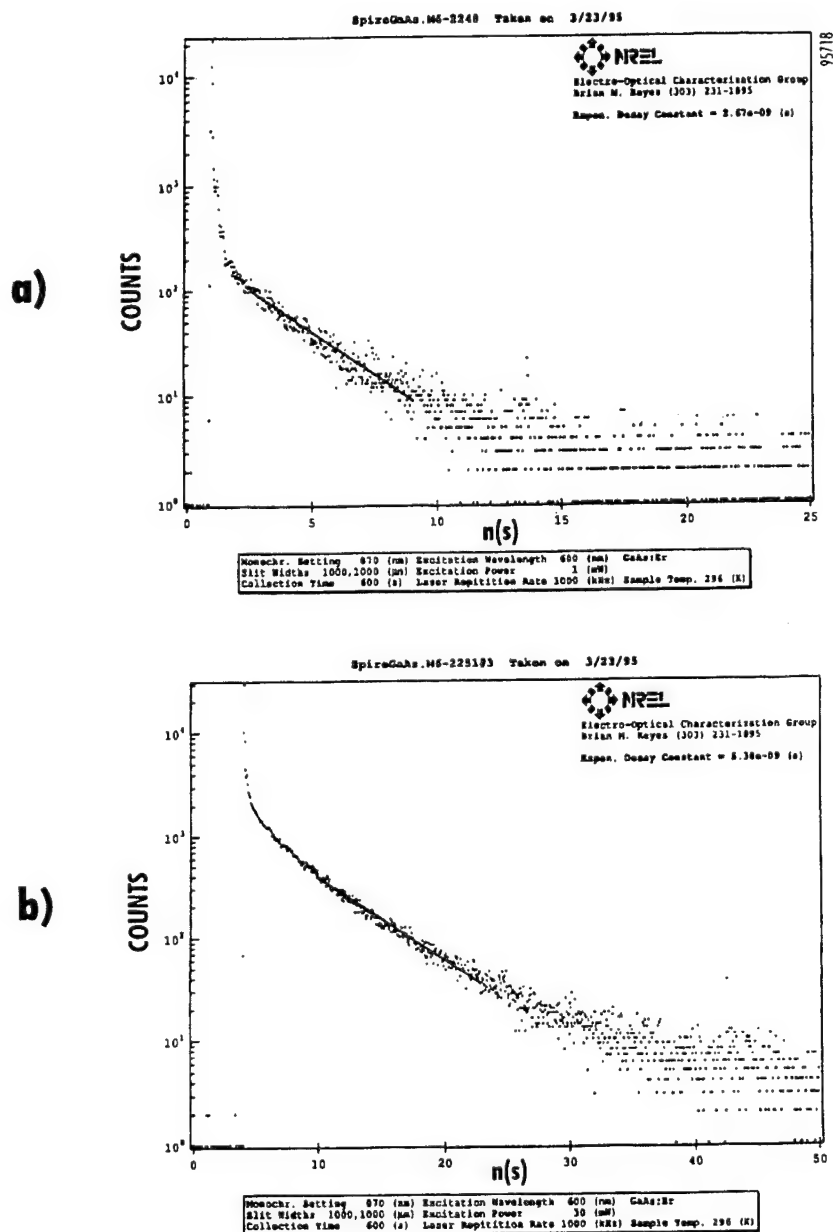
Figure 31   *Minority carrier lifetime measurements, courtesy of NREL, on erbium doped GaAs material showing very faster carrier recombination (<100 ps) with (top, sample 2248, laser structure) and without (bottom, sample 2251)surface passivation.*

2.4.2   Electrical and Optical Characterization of Erbium-Doped GaAs Diodes

Material prepared for diode fabrication had the structure shown in Figure 22. Three wafers were used to make the diodes. One wafer (2249) was of the type "A" in Figure 22, without erbium doping. This material produced working 970 nm lasers and was used as a base line for the erbium doped samples. A second wafer (2248) had the same structure "A" but with the indicated erbium doping. The third wafer (2258) had the structure shown in Figure 22 "B". Here, the N- and P-type doping was reduced in the region nearest the quantum well to reduce predicted self-absorption of the outgoing light.

Spire made LEDs from these wafers, saving some material so as to be able to fashion lasers, if desirable. It was believed that LEDs would have a greater chance of operating correctly as the lasers needed additional processing, with a greater chance for yield loss not due to the change in dopant. The LEDs from the wafer without erbium functioned normally, as expected, emitting 970 nm light (Figure 32a). These devices, as well as all of the erbium doped diodes, also emitted near IR light (Figures 32b and 32c) characteristic of the GaAs substrate material. The erbium doped diodes had no detectable emission at the expected 1.54 micron. They were tested at both 300 and 77K.

Electrical parameters for these LEDs are shown in Figure 33. The device without erbium looks like a near perfect diode with large sharp reverse breakdown voltage and low series resistance in the forward direction. Devices fabricated form sample wafer number 2248, with erbium doping, show large series resistance in the forward direction, indicating contact problems, and leakage current in the reverse direction. Devices from sample wafer 2258 had lower series resistance in the forward direction than 2248, implying that the possible contact problem is not related to the erbium doping. However, this last sample also has high leakage currents, which are attributed to the erbium doping at this time.

At the conclusion of the LED experiment, laser diodes were fabricated from samples 2248, 2461, and 2463. Sample 2461 was nominally an exact copy of wafer from run 2249 without added erbium doping, while sample 2463 was a similar to wafer 2248 but with erbium doping on only one side of the quantum well - the silicon or "N" type dopant side. The sample without erbium was included as a control, we expected to fabricate good 970 nm lasers. The sample with erbium on only one side of the quantum well was a concession to the presence of silicon doping with the erbium dopant. At the given deposition temperature the extra dopant should not affect the operation of the diode, if it were confined to the erbium included layer.

All lasers were fabricated according to Spire's proven process which resulted in the 970 nm lasers, Table 4 . The diodes from run 2461 without erbium had very good current-voltage curves Figure 34), but did not emit any light. This was in spite of photoluminescence testing prior to device fabrication which showed appropriate signals. Emission of light at any wavelength, from 800 (GaAs signals) to upwards of 1600nm was not detected from any of these devices. We have no explanation.
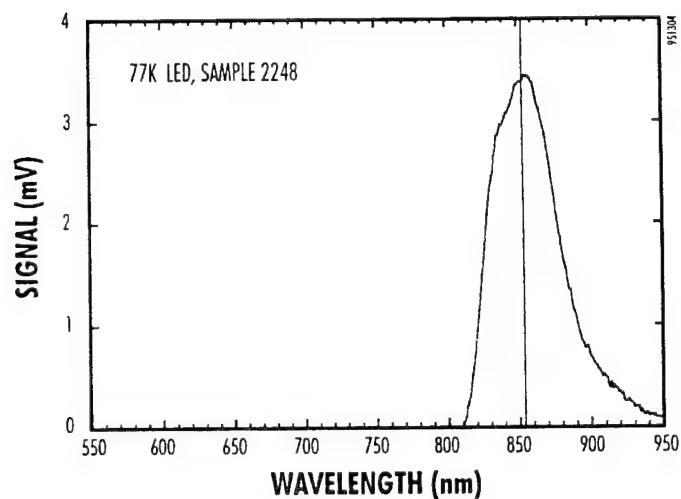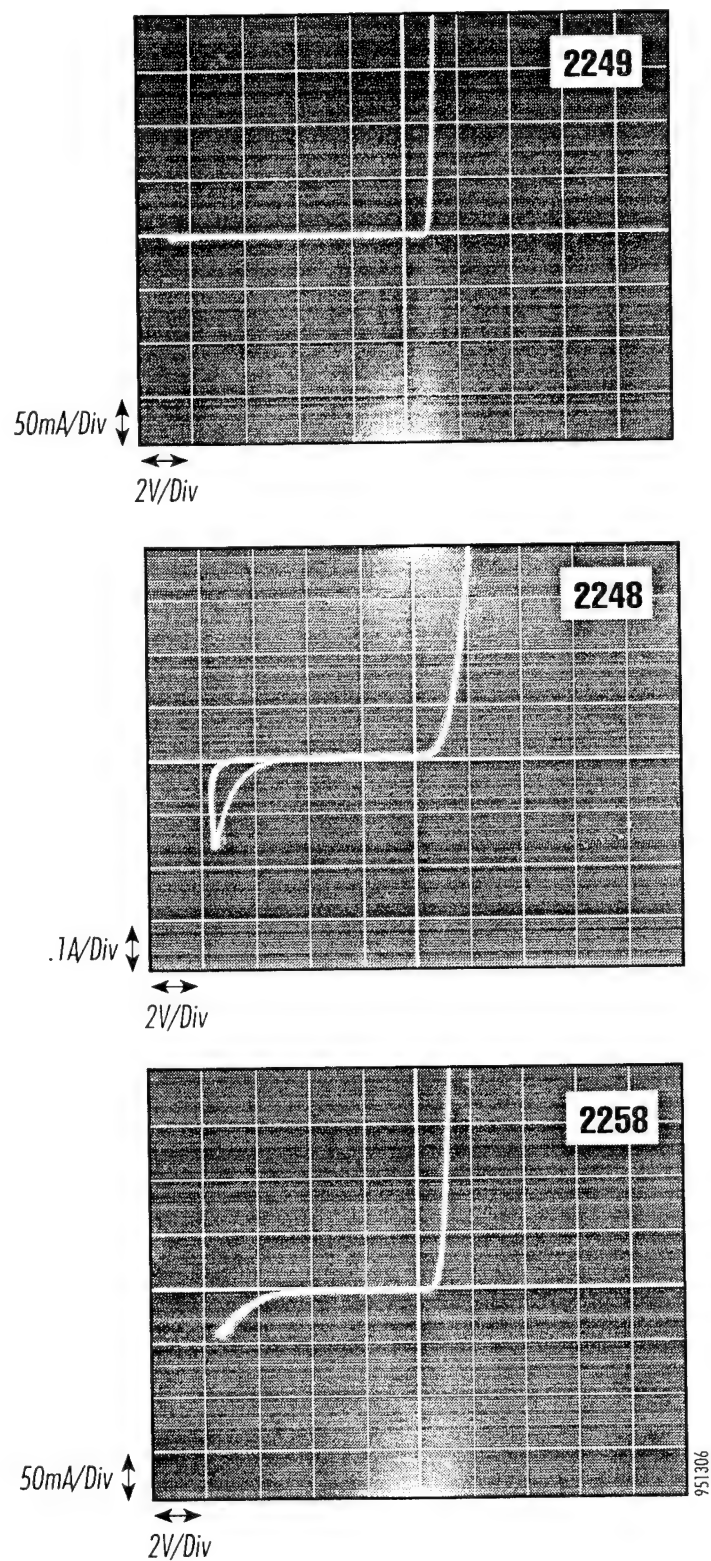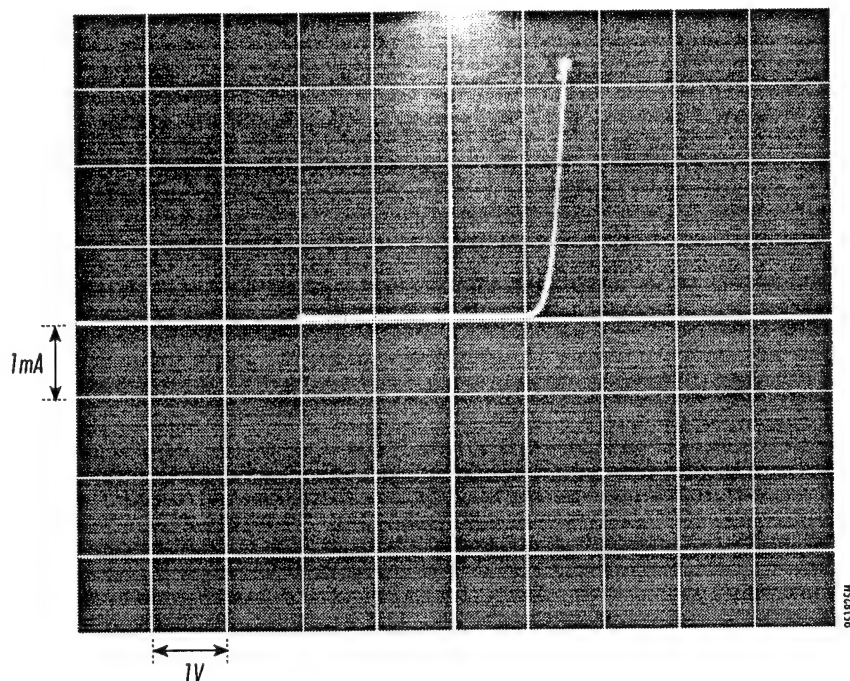
36
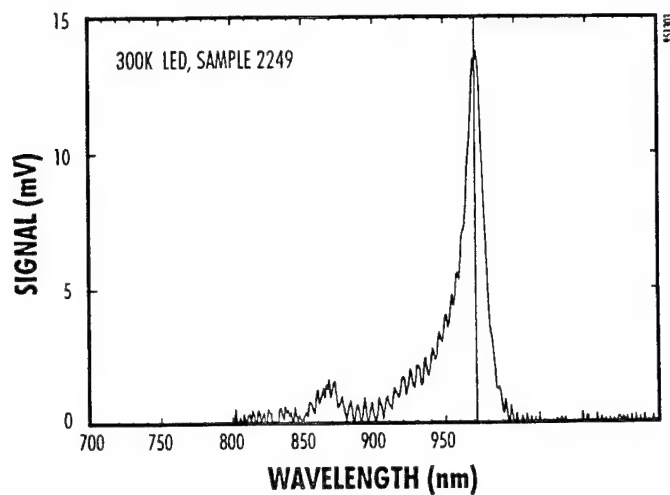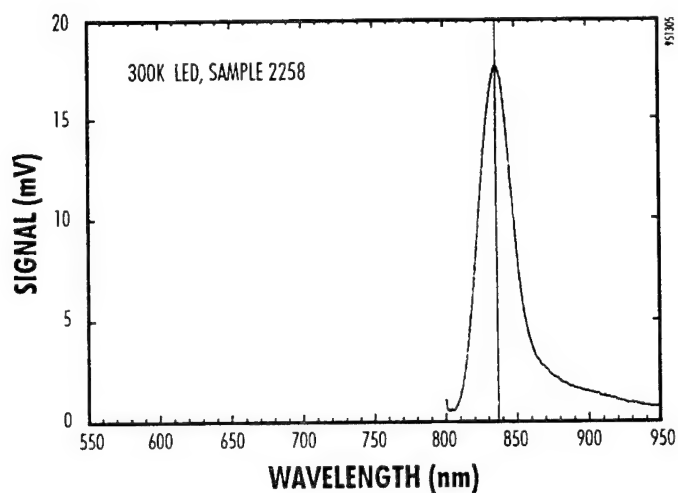
Figure 32   *Electroluminescence from GaAs LEDS, sample 2249: a) without erbium; samples 2248 b) and 2258 c) with erbium. Note changes in relative scale.*

Figure 33   *Representative I-V characteristics of LEDs from 2249 (no erbium) and samples 2248 and 2258 with erbium. All were good diodes but the erbium doped devices had high leakage currents.*

38

Figure 34   *I-V characteristic of laser diode from wafer 2461, nominal duplicate of wafer 2249.*

2.5   Design and Fabricate a GaAs-Based Diode-Laser Coupled to an Er-doped Waveguide

The concept for this device is to begin with a structure similar to that of Figure 22b, and to etch off the top conductive layers in a patterned area, exposing the GaAs waveguide around the quantum well. The device would then be ion implanted with a light mass ion such as carbon, oxygen, and/or fluorine. The implant would not penetrate the capping layers over the laser, but would destroy the quantum well in the region where these layers had been removed. The implanted ions increase the PL emission of erbium doping. In theory, this device works like a monolithically integrated, end pumped cavity laser. Close coupling between the implanted waveguide region and the actual pumping laser should improve overall efficiency compared to separate diode lasers and microcavities.

Work on this task started with ion implantation of erbium doped layers (samples 2256 and 2246) to optimize choice of ion specie and dose. Samples were cut into four pieces and implanted according to the schedule shown in Table 8. All pieces were then annealed in a hydrogen- 2% arsine atmosphere at 53 torr at 800°C for twenty minutes. The PL signal from all ion-implanted samples was reduced by more than a factor of ten compared to the signal of untreated pieces (Table 8). However, that piece of sample 2256 which was annealed but not ion-implanted showed an increase in PL signal of about a factor of ten (Figure 35). The increase in PL at room temperature for the annealed sample was even greater (Figure 36).

Table 8   *Ion implantation conditions.*

| Sample ID	Ion Specie	First Implant		Second Implant	
		Energy (KV)	Dose (cm^{-2})	Energy (KV)	Dose (cm^{-2})
2246-1	$_{12}C^+$	190	5×10^{15}	50	1.25×10^{15}
2246-2	$_{12}C^+$	190	2×10^{16}	50	5×10^{15}
2246-3	$_{12}C^+$	190	1×10^{17}	50	2×10^{16}
2246-4	none	-	-	-	-
2256-5	$_{19}F^+$	190	1×10^{15}	50	2×10^{14}
2256-6	$_{19}F^+$	190	2×10^{15}	50	5×10^{14}
2256-7	$_{19}F^+$	190	1×10^{16}	50	2×10^{15}
2256-8	none	-	-	-	-

The increase in PL is tentatively attributed to diffusion of the dopant erbium moving to more favorable lattice sites for optical activation. Prior to annealing, channeling RBS, Figure 37, showed that only about one-third of the erbium was substitutional. The PL increase could result from increased substitutional percentage, or close coupling to oxygen atoms already present in the lattice.

Two specimens, annealed and unannealed, were examined by transmission electron microscopy (TEM) to elucidate the physics behind the increase in PL with annealing. The work was performed by Brian Demczeck at the Rome Air development Center at Hanscom AFB, MA.

He reported that no obvious changes could be discerned between the heat treated and untreated samples. However, the image of the annealed sample "fluctuated" in brightness. Such behavior was observed only in ferroelectric materials by the microscopist. Spire believed that the increase in PL could be due to the formation or break-up of precipitates of erbium-arsenide as had been reported for highly doped GaAs samples.[16] Such structures were not observed in this work. TEM microphotographs are not available.

2.6   PLE of Erbium Doped GaAs

A very important clue to the mechanism for excitation of erbium in GaAs was revealed by combined photoluminescence (PL) and photoluminescence-excitation (PLE) spectra from samples 2251 and 2254. This work was performed by Dr. Nancy Haegel of Fairfield University. These samples were 0.5 μm of erbium doped GaAs grown epitaxially on a buffer layer of AlGaAs on GaAs. Sample 2251 was grown at 500°C and sample 2254 was grown at 550°C.
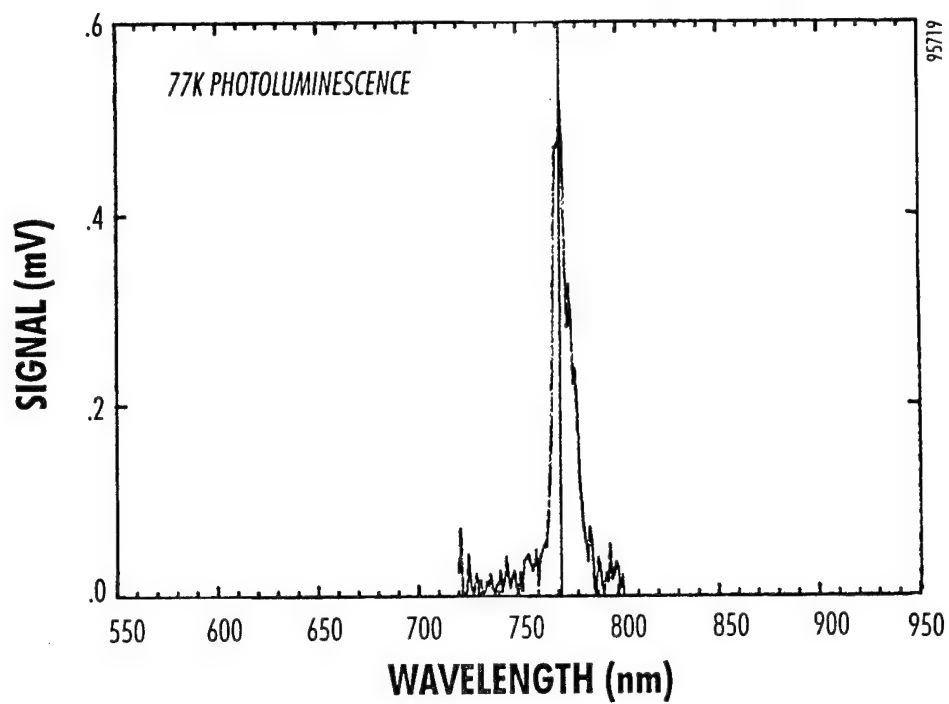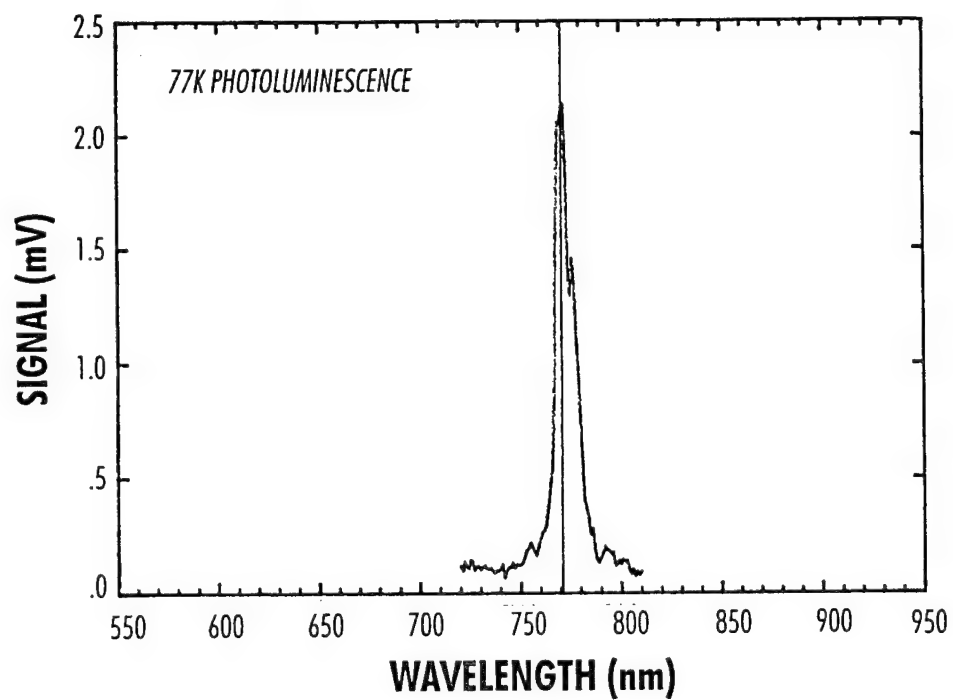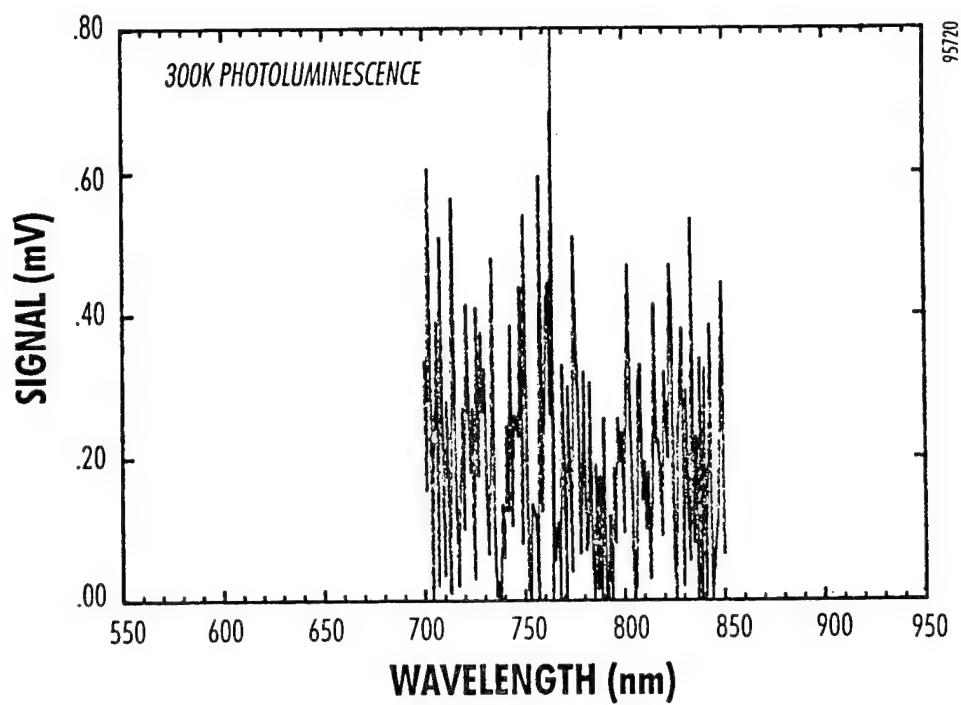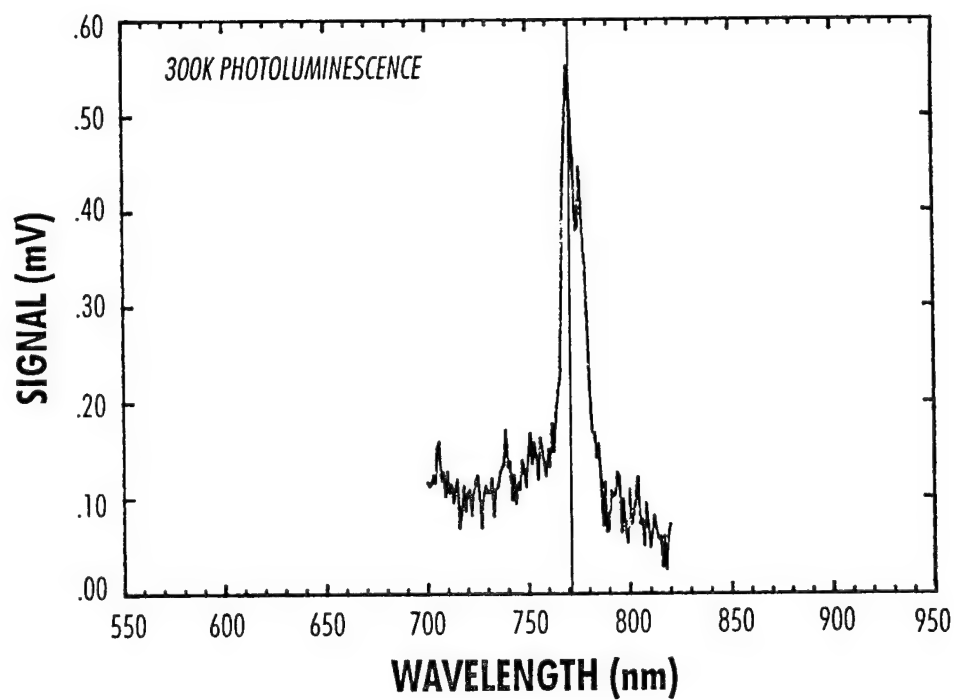
Figure 35   *PL at 77K of unimplanted sample 2256 a) before annealing and b) after annealing.*

41

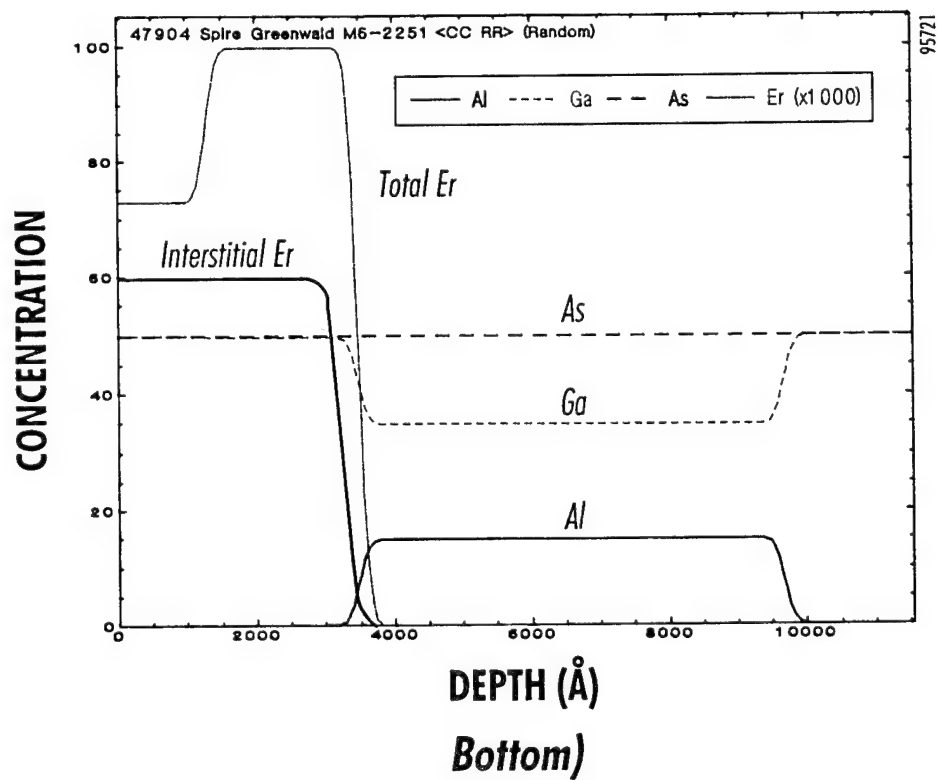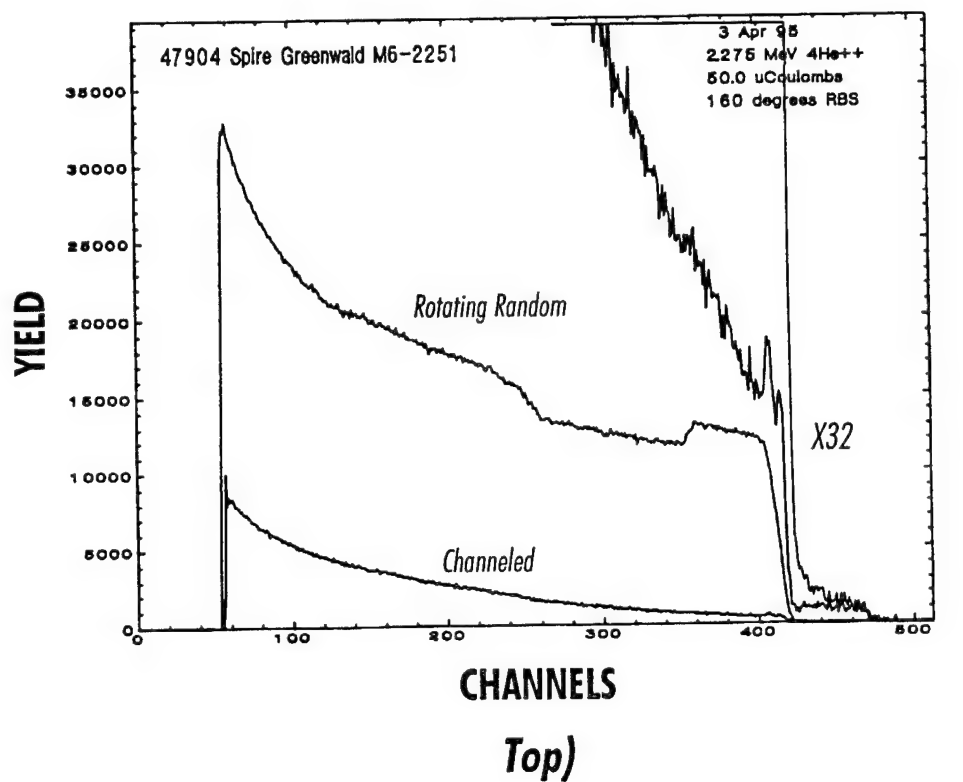**Figure 36**   *PL at 300K of unimplanted sample 2256 a) before, and b) after annealing.*

Figure 37 *Channeling RBS data for sample 2251 (top) and calculated elemental distribution (bottom).*

The PL spectra taken at Fairfield with 524 nm excitation are shown in Figure 38. The PL spectra taken at Spire with 488 nm excitation are shown in Figure 26. The peak in Figure 38 appears symmetrical centered at 1538 nm. Spire's data appears to have a secondary peak at slightly longer wavelength, and the main peak is centered at 1544 nm. The relative magnitude between samples 2251 and 2254 are consistent between the two data sets.
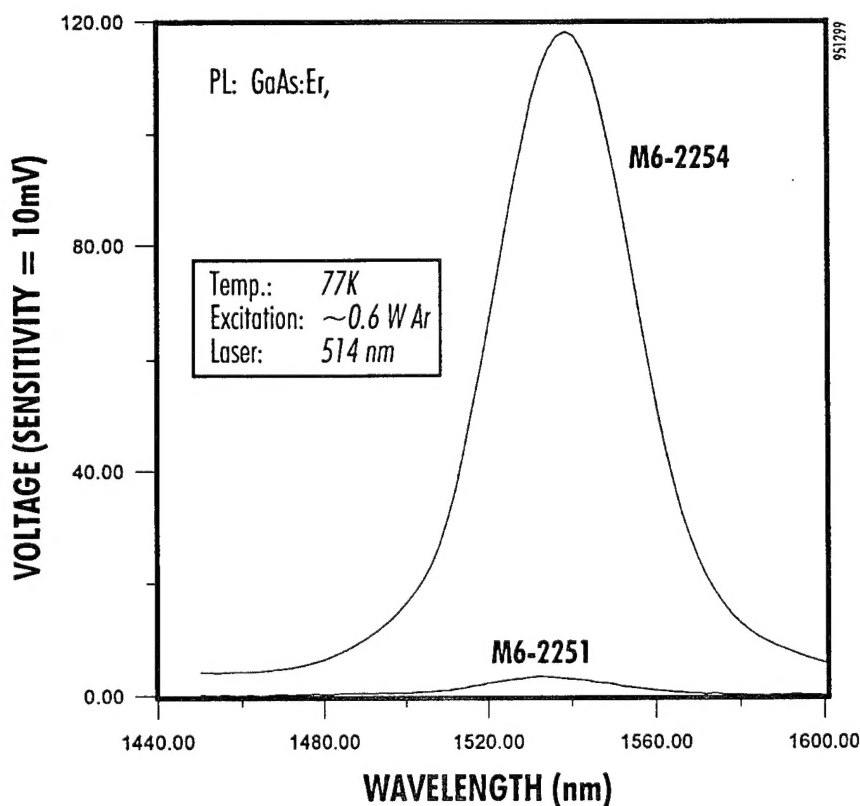

Figure 38 *PL spectra of samples 2251 and 2254 at 514 nm excitation as measured at Fairfield University.*

The PLE spectra is shown in Figure 39. The small peak at 980 nm compared to the cutoff at the GaAs bandgap edge implies that absorption of light by erbium ions directly is negligible compared to absorption of light by the semiconducting host material. Our conclusion is that carriers generated in the host material recombine at the erbium "defect" to generate the PL emission.
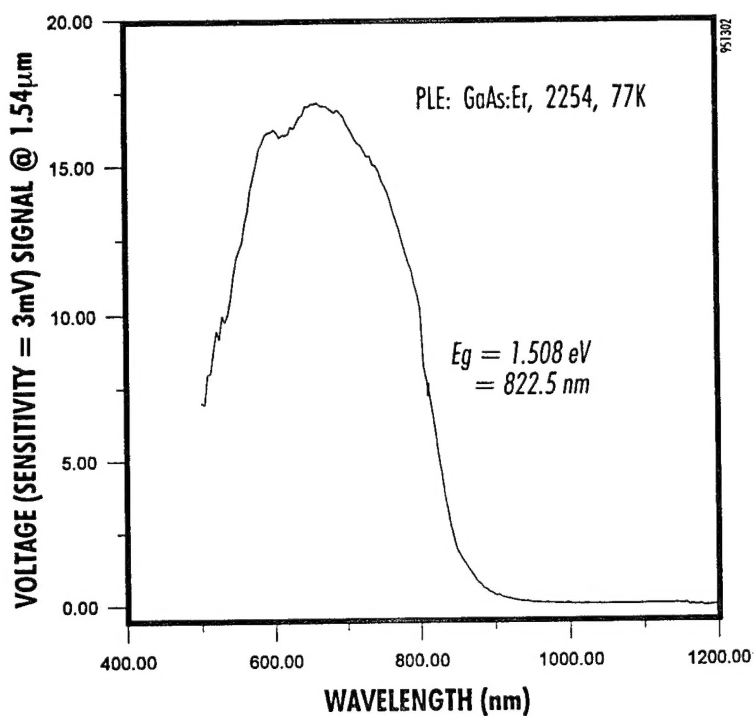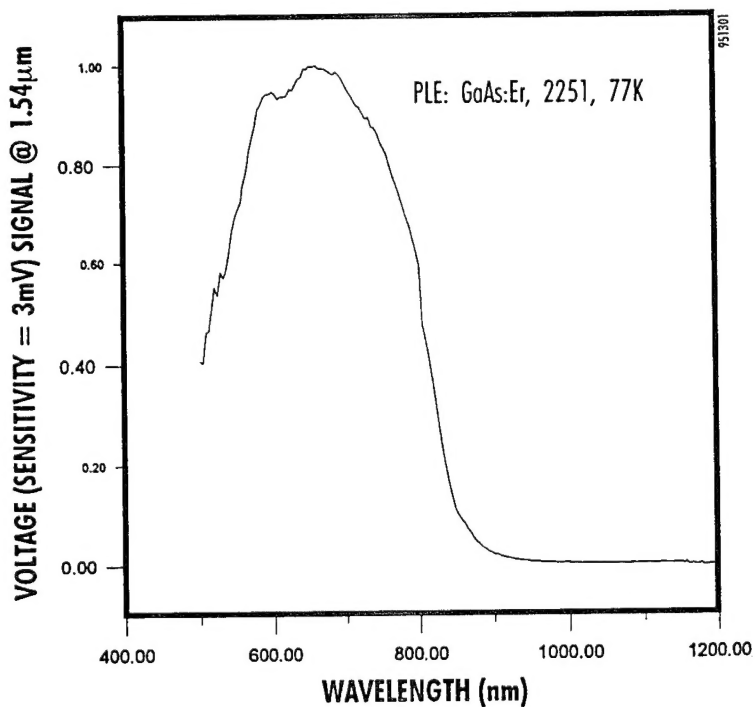
Figure 39 *PLE spectrum for samples 2251 and 2254 showing variation in signal at 1.54 μm as a function of wavelength of excitation energy. Note change in vertical scale.*

45

SECTION 3

CONCLUSIONS

We showed that it is possible to add erbium dopant to MOCVD grown, epitaxial layers of GaAs and/or AlGaAs without carbon or oxygen contamination. This was accomplished with the use of new metalorganic chemicals developed through this research.

We also showed that good PL and cathode luminescence could be obtained from these layers. Most importantly, we showed that the cause of the PL was most likely excitation from electron-hole pair recombination at the defect site in GaAs. The PL signal from excitation light shorter than the bandgap of the host material was very much larger than the PL signal from any expected absorption directly by the erbium ions (at 980nm, for example). This data implied that the indirect semiconductor laser with an erbium waveguide is not very efficient. Direct excitation by carriers from electrical pumping of the defect did not give rise to detectable emission signals in this study.

SECTION 4

REFERENCES

1. M. Kushibe *et. al.*, U. S. Patent 4,928,285 (1990), assignee Toshiba.
2. S. J. Chang and K. Takahei, *Appl. Phys. Lett.* **65**, 433 (1994).
3. H. Ennen *et. al.*, *J. Appl. Phys.*, **61**, 4877 (1987).
4. T. Bennyattou *et. al.*, *Appl. Phys. Lett.*, **60**, 350 (1992).
5. D. W. Elsaesser *et.al.*, *J. Crystal Growth,* **127**, 707 (1993).
6. Kunihiko Uwai *et. al.*, *Appl. Phys. Lett.* **51**, 1010 (1987); also, by same authors: *J. Crystal Growth*, **93**, 583 (1988).
7. Xiao M. Fang, *et. al.*, Mat. Res. Soc. Symp. Proc., **301**, 15 (1993);
   also by same authors: *J. Appl. Phys.* ,**74**, 6990 (1993);
   also by same authors: *J. Electronic Mat.*, **23**, 1269 (1994).
8. K. Takahei, *et. al.*, *J. Appl. Phys.*, **76**, 4332 (1994).
9. D, C. Gordon, B. A. Vaartstra, T. F. Keuch and J. M. Redwing, "Novel Organoerbium Source Reagents for MOCVD of Erbium Containing Alloys", Final Report for contract NAS3-26708, NASA-Lewis research Center, (1993).
10. A. C. Greenwald, William S. Rees, Jr., and Uwe W. Lay; "MOCVD Erbium Sources" in <u>Rare Earth Doping of Semiconductors</u>, ed. G. S. Pomrenke *et. al.*, Mat. Res. Soc. Symp. Proc. **301**, p21 (Materials Research Society, Pittsburgh, PA, 1993).
11. W. S. Rees, Jr, U. W. Lay and A. C. Greenwald, "Preparation and Characterization of New Source Compounds for Erbium Doping of Semiconducting Materials", in <u>Gas Phase and Surface Chemistry in Electronic Materials Processing</u>. ed. T. J. Mountziaris, *et. al.*, *Mat. Res. Soc. Symp. Proc.* **334**, p207 (Materials Research Society, Pittsburgh, PA, 1994).
12. Oliver Just and William S. Rees, Jr., "Incorporation of Erbium in Semiconducting Materials Employing OMVPE of Various Amide Sources", presentation at <u>Florida Advanced Materials Chemistry Conference</u> , Palm Coast, FL, March 21, 1995.
13. William S. Rees, Jr., "Chemical Issues in Semiconductor Doping", presentation at <u>American Chemical Society National Meeting</u>, Anaheim, CA, April 5, 1995.
14. Oliver Just *et al.*, accepted for publication as a communication in *Angewandte Chemie,* 1995.
15. S. Sethi, *et al.*, *IEEE Electron Device Lett.* **16 (3)**, p.106 (1995).
16. I. Poole *et al.*, *J. of Crystal Growth,* **121,** p121 (1992).